
GAZİ ÜNİVERSİTESİ
Gazi
1926

SEA AND LAND CLUTTER ANALYSIS USING HORIZONTAL AND VERTICAL POLARIZATION ANTENNAS IN X-BAND

Zeynep ALBAYRAK

IN PARTIAL FULFILLMENT OF THE REQUIREMENTS
FOR THE DEGREE OF MASTER OF SCIENCE
IN ELECTRICAL AND ELECTRONICS ENGINEERING DEPARTMENT

GAZİ UNIVERSITY
GRADUATE SCHOOL OF NATURAL AND APPLIED SCIENCES

JUNE 2024

ETHICAL STATEMENT

I at this moment declare that in this thesis study, I prepared the thesis writing rules of Gazi University Graduate School of Natural and Applied Sciences;

- All data, information, and documents presented in this thesis have been obtained within the scope of academic rules and ethical conduct,
- All information, documents, assessments, and results have been presented by scientific ethical conduct and moral rules,
- All material used in this thesis that is not original to this work has been exhaustively cited and referenced,
- No change has been made in the data used,
- The work presented in this thesis is original,

or else, I admit all loss of rights to be incurred against me.

Zeynep ALBAYRAK

25/06/2024

SEA AND LAND CLUTTER ANALYSIS USING HORIZONTAL AND VERTICAL POLARIZATION ANTENNAS IN X-BAND

(M. Sc. Thesis)

Zeynep ALBAYRAK

GAZİ UNIVERSITY

GRADUATE SCHOOL OF NATURAL AND APPLIED SCIENCES

June 2024

ABSTRACT

The radar systems that use horizontal and vertical polarization antennas have several advantages such as having different clutter power and Radar Cross Section (RCS), improving synthetic aperture radar (SAR), and tracking cross-polarization jammer. In this thesis changes in sea and land clutters according to vertical and horizontal polarizations are analyzed using Matrix Laboratory (MATLAB). The angle is between the main beam of radar and the surface defined as the grazing angle. Clutter is defined as the unwanted reflections from the surface on which the target is to be detected. Clutter depends on the frequency, polarization, grazing angle, land type, sea state, wave height, wind velocity, and wind direction. Normalized clutter is shown with σ^0 and is also called a backscatter coefficient. Analyses of clutters are calculated for $0.1^\circ - 10^\circ$ grazing angles, and results are given in σ^0 (in dB) vs grazing angle (in degree) graphs. Analyses of sea clutter performed with Royal Radar Establishment (RRE), Georgia Institute of Technology (GIT), Proposed, and Naval Research Laboratory (NRL) models. Sea clutter is calculated and 1 - 6 sea states. Analyses for land clutter performed with the Ulaby and Dobson model for different land types such as soil & rock, grasses, shrubs, short vegetation, road surfaces, and dry and wet snow. To have comparable results from models, clutters are calculated for X-band (8 - 12 GHz) which is the common band between models. The main findings are using horizontal and vertical polarization antennas provide the changing sea and land clutters. When horizontally polarized electromagnetic (EM) waves are used in radar, less sea clutter is calculated than when vertically polarized ones are used. For land clutter calculations, the polarization type which has less clutter varies for different land types. Therefore, dual-polarization antennas and horizontal polarization ones are used in practical applications. Chilbolton Advanced Meteorological Radar (CAMRa), WR120, Radar Satellite-1 (RADARSAT-1), RM-1290, and FINO-I are examples.

Science Code : 93415
Key Words : Clutter, Royal Radar Establishment, Georgia Institute of Technology, Naval Research Laboratory, Ulaby and Dobson
Page Number : 65
Supervisor : Prof. Dr. Nursel AKÇAM

X-BANTTA YATAY VE DÜŞEY POLARİZASYON ANTENLERİ KULLANILARAK DENİZ VE KARA KARGAŞASI ANALİZİ

(Yüksek Lisans Tezi)

Zeynep ALBAYRAK

GAZİ ÜNİVERSİTESİ

FEN BİLİMLERİ ENSTİTÜSÜ

Haziran 2024

ÖZET

Radar sistemlerinde yatay veya düşey polarizasyon antenleri kullanıldığı durumlarda farklı kargaşa yansıma katsayısı elde edilir. Bu tezde yatay ve düşey polarizasyon antenleri kullanılmasının deniz ve kara kargaşasına olan etkisi farklı modeller kullanılarak incelenecektir. Kargaşa analizleri MATLAB kullanılarak yapılmıştır. Yüzey ile radarın ana hüzmesi arasındaki açıya bakış açısı (grazing angle) denir. Kargaşa, hedef tespiti yapılmaya çalışılan yüzeyden gelen istenmeyen yansımalar olarak tanımlanır. Radarın çalışma frekansına, elektromanyetik dalganın polarizasyonuna, bakış açısına, yüzey türüne bağlı olarak değişir. Ayrıca, deniz kargaşası deniz durumuna, denizdeki dalgaların yüksekliğine, rüzgâr hızına ve rüzgâr yönüne bağlıdır. Kargaşa sinyali radarın aydınlattığı yüzey alanına bağlı olarak değiştiği için sinyal seviyesini analiz etmek üzere "Normalize kargaşa yansıma katsayısı, σ^0" kullanılmaktadır. Bu tezdeki hesaplamalar 0.1 ile 10 derece aralığındaki bakış açısı için yapılmıştır. Deniz kargaşasını hesaplamak için dört model kullanılarak 1 ile 6 arasında değişen deniz seviyeleri için deniz kargaşası hesaplanmıştır. Kullanılan modeller Kraliyet Radar Kuruluşu (Royal Radar Establishment, RRE), Georgia Teknoloji Enstitüsü (Georgia Institute of Technology, GIT), Önerilen (Proposed) ve Deniz Araştırma Enstitüsü (Naval Research Laboratory, NRL) modelleridir. Kara kargaşası için Ulaby ve Dobson modeli kullanılarak toprak ve kaya, çimenler, çalılar, kısa bitki örtüsü, yol yüzeyleri ve kuru ve ıslak kar gibi farklı yer türleri için hesaplamalar yapılmıştır. Modeller arasında karşılaştırma yapabilmek için, modellerin geçerli olduğu ortak frekans bandı olan 8 – 12 GHz (X Bant) seçilmiştir. Ayrıca, kara ve ortalama deniz kargaşası karşılaştırılmıştır. Sonuç olarak yatay polarize anten kullanıldığında daha düşük kargaşa olduğu hesaplanmıştır. Bu sayede radar, daha hedef tespit menzilini artırır. Bu avantajından dolayı pratik uygulamalarda kullanılmaktadır. RADARSAT-1, RM-1290 ve FINO-I radarları örnek olarak verilmiştir.

Bilim Kodu : 93415
Anahtar Kelimeler : Kargaşa, Kraliyet Radar Kuruluşu, Georgia Teknoloji Enstitüsü, Deniz Araştırma Laboratuvarı, Ulaby ve Dobson
Sayfa Adedi : 65
Danışman : Prof. Dr. Nursel AKÇAM

ACKNOWLEDGEMENTS

First, I would like to express my sincere appreciation to my advisor Prof. Dr. Nursel AKÇAM for her continuous guidance. I am deeply thankful for her support and trust during my master's studies. Also, I appreciate her kind patience.

Second, I thank my thesis committee members, Prof. Dr. Özgür ERTUĞ and Dr. Nilay AYTAŞ KORKMAZ for their invaluable comments and insightful recommendations.

Furthermore, I would also like to appreciate the opportunity provided by ASELSAN Inc. to complete my M. Sc. Degree. Especially, I thank Halil ÖZDEMİR for his mentoring from the beginning to the completion of the thesis.

I would like to extend my utmost gratitude to my mother, father, and brother for their unlimited love and support throughout my life.

Last but not least, no words can express my gratitude to Özgür ORAN. I could not achieve this thesis without his endless support.

CONTENTS

Page

Page

LIST OF TABLES

Table **Page**

LIST OF FIGURES

Figure **Page**

Figure **Page**

Figure **Page**

Figure **Page**

Figure **Page**

SYMBOLS AND ABBREVIATIONS

The symbols and abbreviations used in this study are presented below, along with their explanations.

Symbols	Explanations
$\boldsymbol{\delta}$	Grazing angle
$\boldsymbol{\Delta R}$	Range resolution
$\boldsymbol{\lambda}$	Wavelength
$\boldsymbol{\Theta_3}$	3 dB azimuth beamwidth
$\boldsymbol{\sigma^0}$	Backscattering coefficient
$\boldsymbol{\sigma_\Phi}$	Roughness parameter
$\boldsymbol{A_i}$	Interference term
$\boldsymbol{A_u}$	Wind direction dependence term
$\boldsymbol{A_w}$	Sea state dependence term
dB	Decibel
$\boldsymbol{f}$	Frequency
$\boldsymbol{G}$	Antenna power gain
$\boldsymbol{\vec{E}}$	Electric field
$\boldsymbol{h_{av}}$	Average wave height
$\boldsymbol{\vec{H}}$	Magnetic field
Hz	Hertz
$\boldsymbol{L_s}$	System loss factor
$\boldsymbol{P_r}$	Received power
$\boldsymbol{P_t}$	Transmitter power
$\boldsymbol{R_0}$	Radar range
$\boldsymbol{s}$	Sea State
$\boldsymbol{U}$	Wind velocity

Abbreviations	Explanations
CAMRa	Chilbolton Advanced Meteorological Radar

Abbreviations	Explanations
EM	Electromagnetic
GIT	Georgia Institute of Technology
LWC	Liquid Water Content
MATLAB	Matrix Laboratory
MIT	Massachusetts Institute of Technology
NRCS	Normalized Radar Cross Section
NRL	Naval Research Laboratory
RADAR	Radio Detection and Ranging
RADARSAT	Radar Satellite
RCS	Radar Cross Section
RRE	Royal Radar Establishment
SAR	Synthetic Aperture Radar
SCR	Signal to Clutter Ratio
SWH	Significant Wave Height

1. INTRODUCTION

The direction of the electric field defines the polarization of electromagnetic (EM) waves. There are two types of polarizations [1]:

- If the directions of the electric field ($\vec{E}$) and magnetic field ($\vec{H}$) are in fixed planes, the wave is linearly polarized. When an electric field moves in a horizontal plane, the electromagnetic wave is horizontally polarized. In the case of vertically polarized, the electric field moves up and down in the vertical plane (Figure 1.1).
- If the directions of the $\vec{E}$ and $\vec{H}$ change with time, it is elliptically polarized. In this type of polarization, there is an arbitrary phase between the vertical and horizontal components of the electric field.

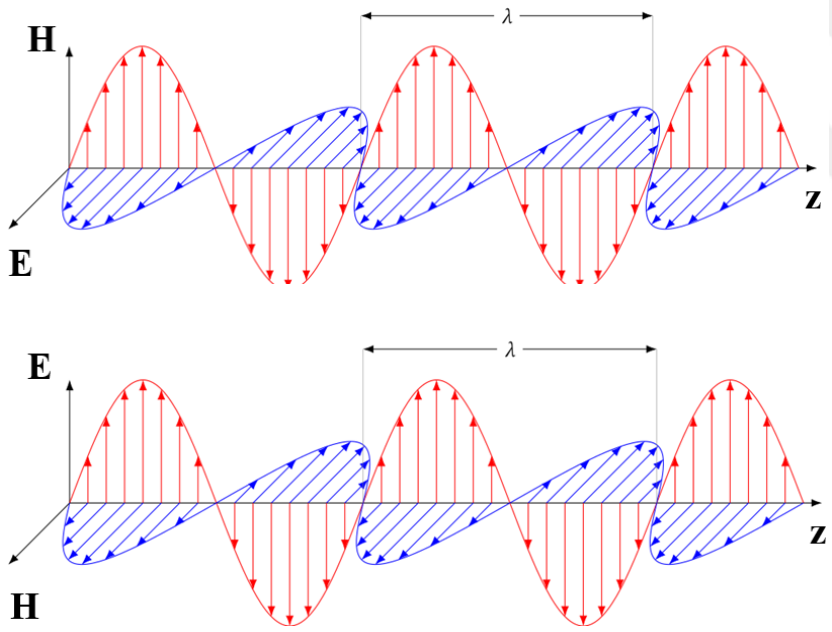

Figure 1.1. Horizontally and vertically polarized electromagnetic waves, respectively and wavelength (λ) [2].

Surface clutter is defined by radar cross section per unit area of the surface that leads to clutter. It is called the backscattering coefficient, reflectivity, clutter coefficient, or clutter depending on interests [3]. It differs from noise being proportional to the amplitude of the transmitted radar signal level, varying with frequency, environmental conditions, and range resolution [4]. To symbolize the backscattering coefficient σ^0 is used. It depends on land type, grazing angle, radar frequency, and polarization [5]. Also, the backscatter coefficient

of the sea depends on the sea state, wind speed, wind direction relative to the look angle of the radar, and wave height [6]. Sea state describes the sea and ocean surface roughness. Douglas sea state that is used in models is given in Table 1.1 with description, wind speed, and significant wave height (SWH).

Table 1.1. Douglas sea state [7]

Douglas Sea State	Description	Wind Speed (knots)	Significant Wave Height (feet)
1	Smooth	0 – 6	0 – 1
2	Slight	6 – 12	1 – 3
3	Moderate	12 – 15	3 – 5
4	Rough	15 – 20	5 – 8
5	Very rough	20 – 25	8 – 12
6	High	25 – 30	12 – 20

The unit of σ^0 is $\frac{m^2}{m^2}$ in linear scale; hence, it is dimensionless. In the dB scale, it is represented with $dB\frac{m^2}{m^2}$, or simply with dB. It is also called normalized radar cross-section (NRCS) [8].

A maritime radar observes EM waves that are reflected from the sea surface in addition to reflected waves from the target. These additional signals are usually unwanted signals and are known as sea clutter. If the power of sea clutter waves is comparable with the power of reflected waves from the target, the signal-to-clutter ratio (SCR) will be low which is not enough to detect the target on the sea surface [9].

Radio Detection and Ranging (RADAR) that is performed to detect a target on land receives reflections from objects such as soil, rock, grass, shrubs, roads, and snow. These reflections are known as land clutter, and they are unwanted since they mask the signal while the radar is trying to detect the target. The performance of target detection of radar deteriorates because of clutter [10].

The angle between the surface and the axis of the main beam is defined as the grazing angle [11]. It is shown in Figure 1.2. As the grazing angle changes, clutter also changes.

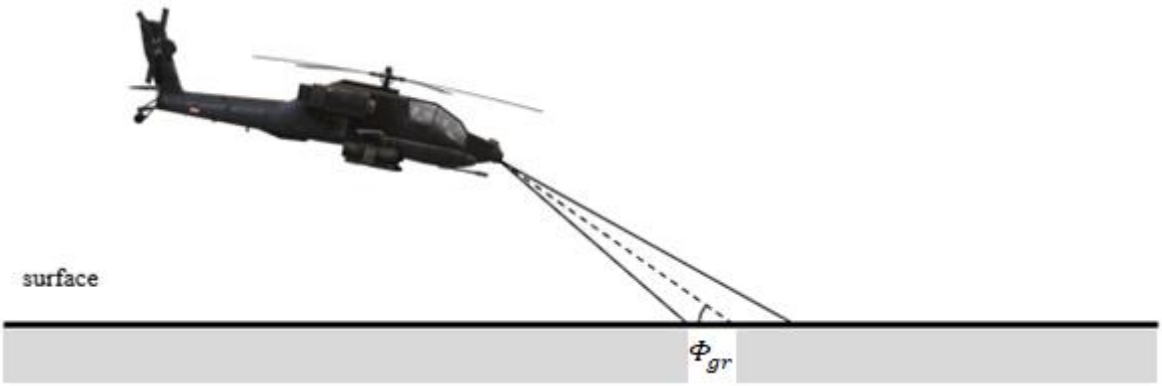

Figure 1.2. Grazing angle between the surface and the middle of the main beam

Several models are developed to calculate clutter. They are based on theoretical approximations of the environment or empirical measurements. They usually give a typical, average, or normalized backscatter coefficient [12]. They may into account land type, grazing angle, polarization, and frequency.

Some of the applications of dual-polarization usage on radar systems are:

- Chilbolton Advanced Meteorological Radar (CAMRa)
  It has a 25 m diameter dish antenna, and it is shown in Figure 1.3. It transmits alternately horizontally and vertically polarized EM waves and receives both co-polarization and cross-polarization returns [13].

Figure 1.3. CAMRa radar system

- Compact Dual Polarimetric X-band Doppler Weather Radar: WR120
  It is produced by Furuno Norge to compensate for the rain intensity loss. It recovers the attenuation due to rain and gives accurate measurements compared to single polarization.

Also, it classifies the particles as hail, snow, and rain [14]. The radar is at the top of a building as shown in Figure 1.4.

Figure 1.4. Furuno's meteorological monitoring and analysis system

Furthermore, the advantages of using a dual-polarization weather radar are explained on Furuno's website [15]. It provides forecasters the better estimations for the target's size, shape, and variety. Secondly, it recovers signal loss due to heavy rain. Thirdly, it is used to recognize the target as snow, hail, or rain. Also, it detects the layer called as melting layer. In this layer snow and ice crystals reach the temperature above the freezing point and they start to melt. Finally, it reduces the sea clutter as will be explained in this thesis.

Some of the applications of horizontal polarization usage on radar systems are:

- RADARSAT-1

  It is used to detect ships. Detection by using horizontal polarization is preferred since horizontal polarization has lower clutter than vertical polarization. Hence, synthetic aperture radar (SAR) has the ship-sea contrast in the imagery. Figure 1.5 shows the

image enhancement of ship detection by comparing the horizontal and vertical polarization waves for the same area [16].

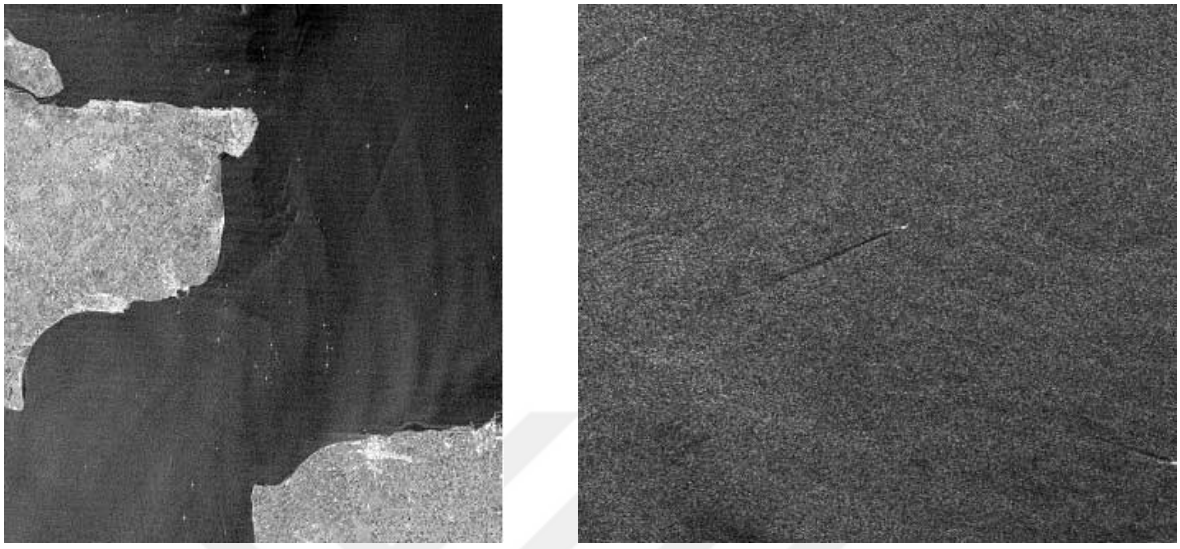

Figure 1.5. RADARSAT-1 images that use horizontal and vertical polarizations

- RM-1290

  It is a marine radar that uses horizontally polarized waves to measure wind direction. Frequency of the radar is in the X-band. A mounted radar is shown in Figure 1.6 [17].

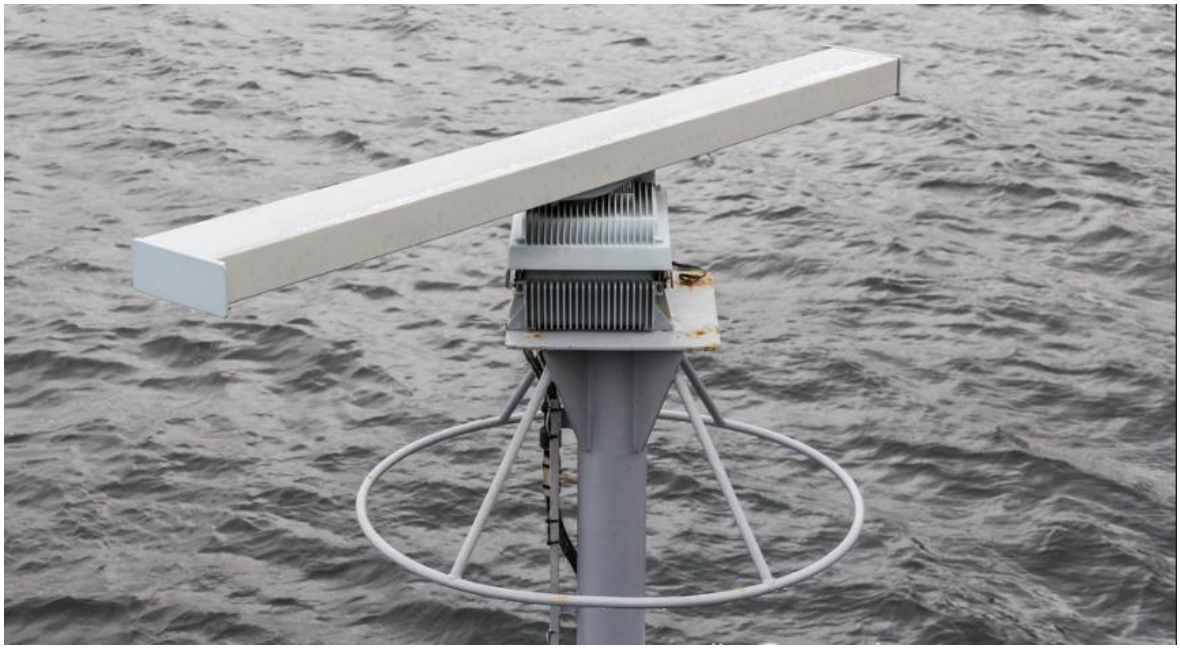

Figure 1.6. RM-1290 radar mounted above sea

- FINO-I

  It is a marine radar to measure wind velocity. It uses horizontally polarized waves to image the ocean surface with trustable information about the velocity of ocean winds [18]. Its platform is shown in Figure 1.7 [19].

Figure 1.7. FINO-I platform with measurement mast that is ~100 m

In this thesis, four models are used to calculate sea clutter. They are depending on frequency, polarization, sea state, and grazing angle. Also, one model is used to calculate land clutter depending on land type besides frequency, polarization, and grazing angle. To achieve that, NRCS is calculated numerically for each case and the results are given in grazing angle vs σ^0 in dB. Since the X band (8 – 12 GHz) is the common band between the models, it is used in analyses to compare the results. Calculations are made using MATLAB for $0.1^\circ - 10^\circ$ grazing angles. Results are compared with the expected results in the literature.

A brief outline of the thesis is given below.

In the first chapter basic definitions and introductions related to EM waves, radar, and clutter are given. In addition, the measure of clutter amplitude, i.e., the NRCS parameter, and parameters affecting it are introduced. Then, examples of practical applications of using dual polarization are listed.

In the second chapter sea clutter is calculated. It is calculated for different sea states between 1 and 6. Moreover, parameters that are used in models are presented in this chapter. In addition, comparisons according to polarizations, models, sea states, and grazing angles are given in this chapter.

In the third chapter land clutter is calculated for different land types which are soil and rock, grass, shrub, short vegetation, road surfaces, and dry and wet snow. Also, comparisons according to polarizations and grazing angle are given.

In the fourth chapter, a brief conclusion is given according to the calculation results. Also, differences and future work are explained.

2. SEA CLUTTER

Sea clutter is the unwanted signal that is backscattered from the sea surface. Polarization of the transmitted wave affects the clutters of the sea.

There are several models to calculate the sea clutter scattering coefficient in terms of polarization, frequency, grazing angle, and sea states. In this thesis four of them will be examined. They are the Royal Radar Establishment (RRE), Georgia Institute of Technology (GIT), Proposed, and Naval Research Laboratory (NRL) models. Clutter is calculated for a $0.1^{\circ} - 10^{\circ}$ grazing angle. Results are also given numerically in Table 2.2 (Section 2.4).

2.1. RRE Model

These should Royal Radar Establishment model was released in the 1970s in the United Kingdom (UK) by using data from [20] and [21]. It has been used for 30 years in the UK to evaluate airborne radar performance. This model is valid for X-band radar frequency and grazing angles which are smaller than 10°. It gives the normalized clutter RCS in dB. To calculate σ^0, it uses polarization type, sea states, and grazing angles. Expressions of the model are [22]:

$$\sigma^0 = a[s] + b[s] * log_{10}(\frac{180*\Phi_{gr}}{\pi}) \text{ if } \Phi_{gr} \leq \frac{\pi}{180} = 1^{\circ} \quad (2.1)$$

$$\sigma^0 = a[s] + c[s] * log_{10}(\frac{180*\Phi_{gr}}{\pi}) \text{ if } \Phi_{gr} > \frac{\pi}{180} = 1^{\circ} \quad (2.2)$$

where s is the sea state (s = 1 to 6), Φ_{gr} is the grazing angle in degrees, and constants used in this model

$$a_{HH}[s] = [-52.0,\ -46.0,\ -42.0,\ -39.0,\ -37.0,\ -35.5] \quad (2.3a)$$

$$b_{HH}[s] = [21.0, 17.5, 12.5, 10.5, 7.0, 3.5] \quad (2.3b)$$

$$c_{HH}[s] = [1.015, 3.39, 2.03, 1.35, 2.03, 2.37] \quad (2.3c)$$

$$a_{VV}[s] = [-51.5, -45.5, -41.0, -38.5, -36.0, -34.5] \quad (2.3d)$$

$$b_{VV}[s] = [15.0, 12.0, 11.5, 11.0, 9.5, 8.0] \quad (2.3e)$$

$$c_{VV}[s] = [8.2, 9.5, 8.0, 7.5, 7.0, 6.5] \quad (2.3f)$$

In the above constants, HH implies that radar transmits and receives horizontally polarized waves. Similar way, VV implies that radar transmits and receives vertically polarized waves.

Calculations in this thesis according to the RRE model and 6 sea states are given in Figure 2.1 – Figure 2.6. In each graph, the normalized clutter is calculated concerning horizontal and vertical polarizations.

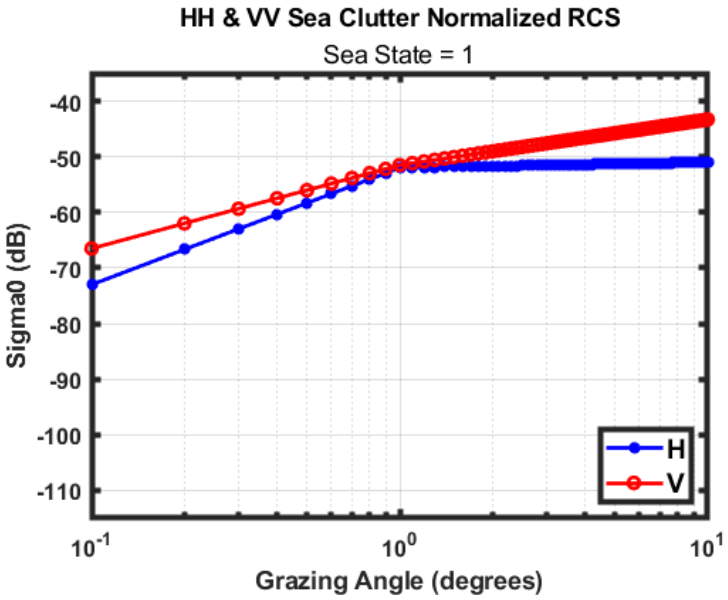

Figure 2.1. HH and VV sea clutter normalized RCS at 10 GHz as a function of grazing angle from the RRE model for sea state 1.

In Figure 2.1, less clutter is calculated for all grazing angles when horizontally polarized waves are used.

As can be understood from the Figure 2.2, horizontally polarized waves have less clutter than vertically polarized ones for all grazing angles.

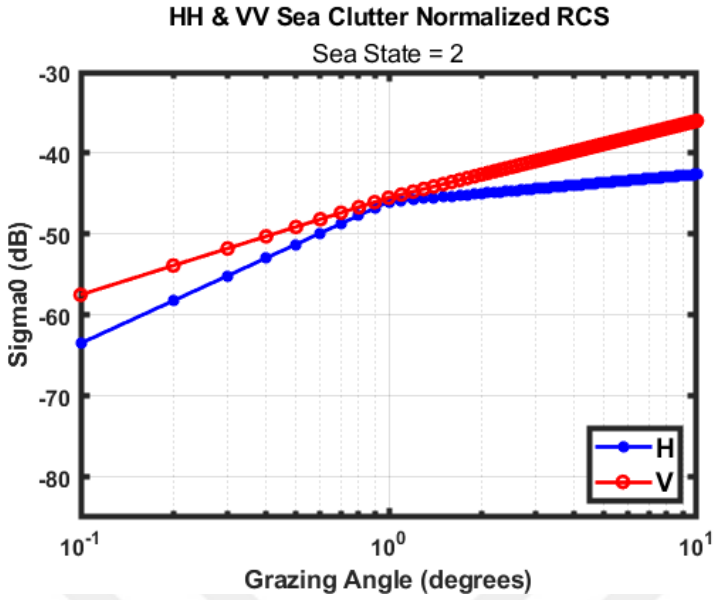

Figure 2.2. HH and VV sea clutter normalized RCS at 10 GHz as a function of grazing angle from the RRE model for sea state 2.

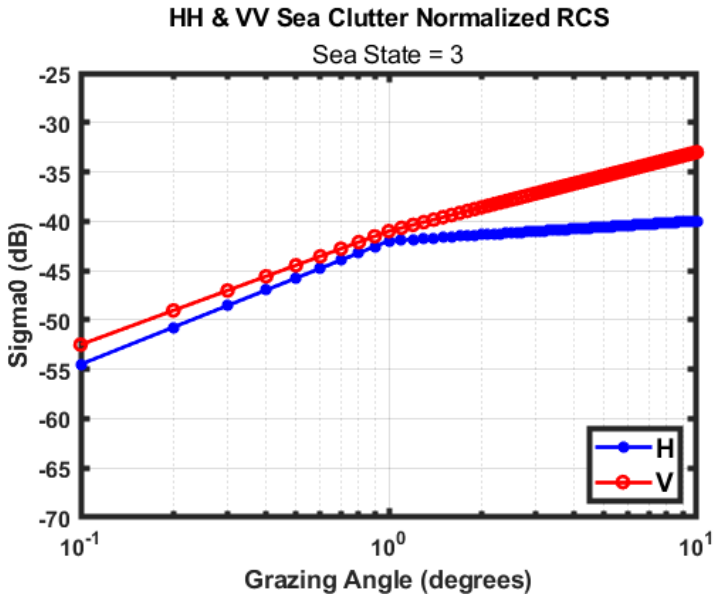

Figure 2.3. HH and VV sea clutter normalized RCS at 10 GHz as a function of grazing angle from the RRE model for sea state 3.

In Figure 2.3, the normalized clutter is calculated for sea state is 3. In the range of $0.1^{\circ} - 10^{\circ}$ grazing angle, the wave that has less clutter is the horizontally polarized wave.

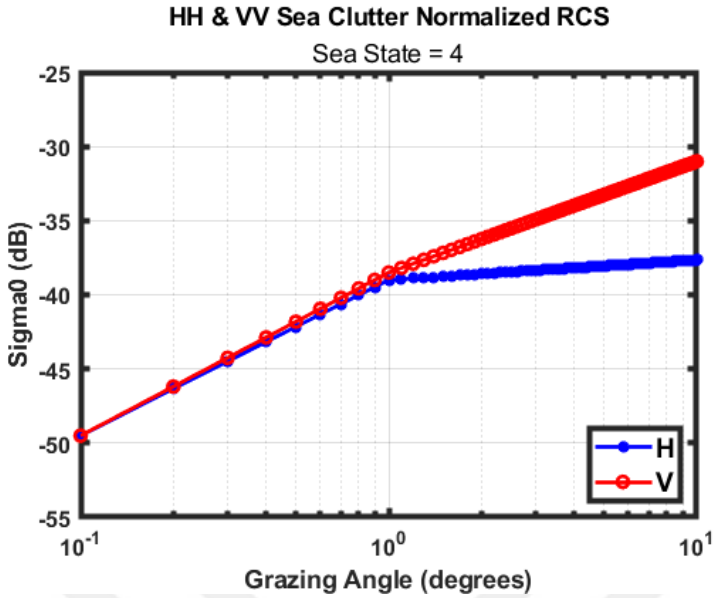

Figure 2.4. HH and VV sea clutter normalized RCS at 10 GHz as a function of grazing angle from the RRE model for sea state 4.

In Figure 2.4, when horizontally polarized waves are used, for all grazing angles less clutter is calculated.

As can be understood from the Figure 2.5, horizontally polarized waves have less clutter than vertically polarized ones for $0.4^{\circ} - 10^{\circ}$ grazing angles. When grazing angle is in the range of $0.1^{\circ} - 0.4^{\circ}$ grazing angles, horizontally polarized waves have more clutter than vertically polarized ones.

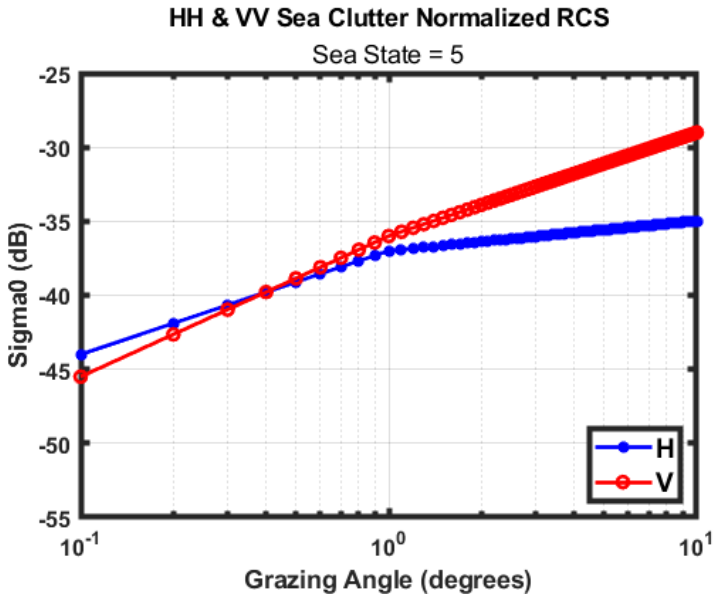

Figure 2.5. HH and VV sea clutter normalized RCS at 10 GHz as a function of grazing angle from the RRE model for sea state 5.

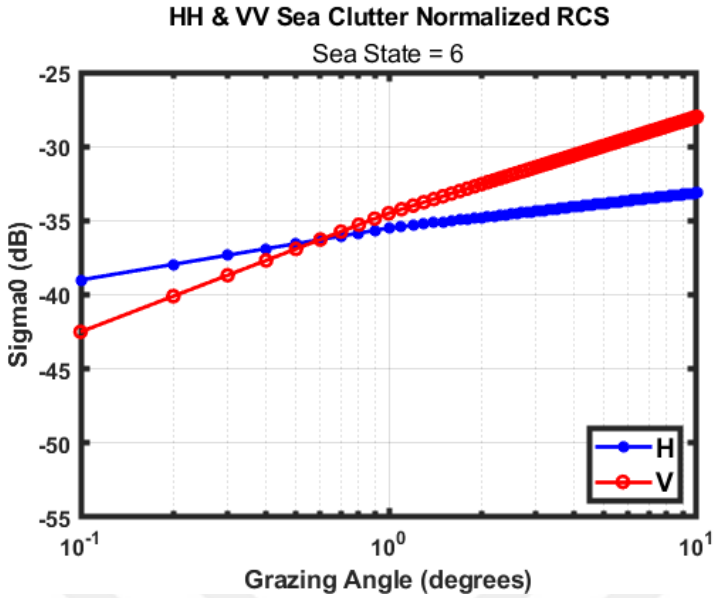

Figure 2.6. HH and VV sea clutter normalized RCS at 10 GHz as a function of grazing angle from the RRE model for sea state 6.

In Figure 2.6, for sea state 6 the normalized sea clutter is calculated and in the range of $0.1^{\circ} - 0.6^{\circ}$ grazing angle, the wave that has less clutter is the vertically polarized wave. On the other hand, vertically polarized waves have less clutter than horizontally polarized ones in the range of $0.6^{\circ} - 10^{\circ}$ grazing angles.

2.2. GIT Model

The Georgia Institute of Technology (GIT) model was released in the 1970s to calculate σ^0 concerning sea state, wind velocity, wave height, and polarization. This model is valid for 1 - 100 GHz frequencies [23]. Expressions of the model are [24]:

$$U = 3.16 * s^{0.8} \tag{2.4}$$

where U is the wind velocity and s is the sea state.

$$h_{av} = 0.00452 * U^{2.5} \tag{2.5}$$

where h_{av} is the average wave height in m.

Define a roughness parameter

$$\sigma_{\Phi} = (14.4 * \lambda + 5.5)\frac{h_{av} * \Phi_{gr}}{\lambda} \tag{2.6}$$

where λ is the radar wavelength in m.

Evaluate an interference parameter by using the roughness term

$$A_i = \frac{{\sigma_\Phi}^4}{1+{\sigma_\Phi}^4} \tag{2.7}$$

The wind direction dependence term

$$A_u = \exp\left(0.2 * \cos(\theta_w) * \left(1 - 2.8 * \Phi_{gr}\right) * (\lambda + 0.015)^{-0.4}\right) \tag{2.8}$$

where θ_w is the angle between the wind and radar look directions in degree.

The sea state dependence term

$$A_w = \left(\frac{1.94*U}{1+\frac{U}{15.4}}\right)^{\frac{1.1}{(\lambda+0.015)^{0.4}}} \tag{2.9}$$

Finally, σ^0 for two polarizations

$$\sigma^0_{HH} = -54.09 + 10 * \log_{10}(\lambda * {\Phi_{gr}}^{0.4} A_i A_u A_w) \tag{2.10a}$$

$$\sigma^0_{VV} = \sigma^0_{HH} - 1.05 * \ln_e(h_{av} + 0.015) + 1.09 * \ln_e(\lambda) + 1.27 * \ln_e\left(\Phi_{gr} + 0.0001\right) + 9.7 \tag{2.10b}$$

Table 2.1. The average wave height and wind velocity according to sea state

s	U	h_{av}
1	3.16	0.08
2	5.50	0.32
3	7.61	0.72
4	9.58	1.28
5	11.45	2.06
6	13.25	2.89

By using the above expressions, calculated average wave height, and wind velocity values are given in Table 2.1. As expected, they both increase as the sea state is increasing.

Calculation results according to the GIT model and 6 sea states are given in Figure 2.7 – Figure 2.12. In each figure, horizontal and vertical polarizations are concerned while calculating the normalized sea clutter for $0.1^\circ - 10^\circ$ grazing angle.

In Figure 2.7, σ^0 is calculated for sea state is 1. For the whole calculation range, i.e. $0.1^\circ - 10^\circ$, horizontally polarized waves have less clutter than vertically polarized ones.

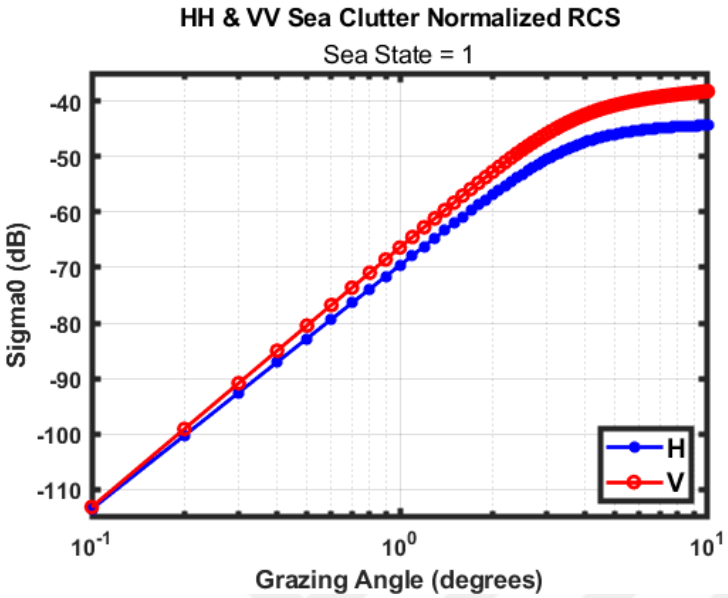

Figure 2.7. HH and VV sea clutter normalized RCS at 10 GHz as a function of grazing angle from the GIT model for sea state 1.

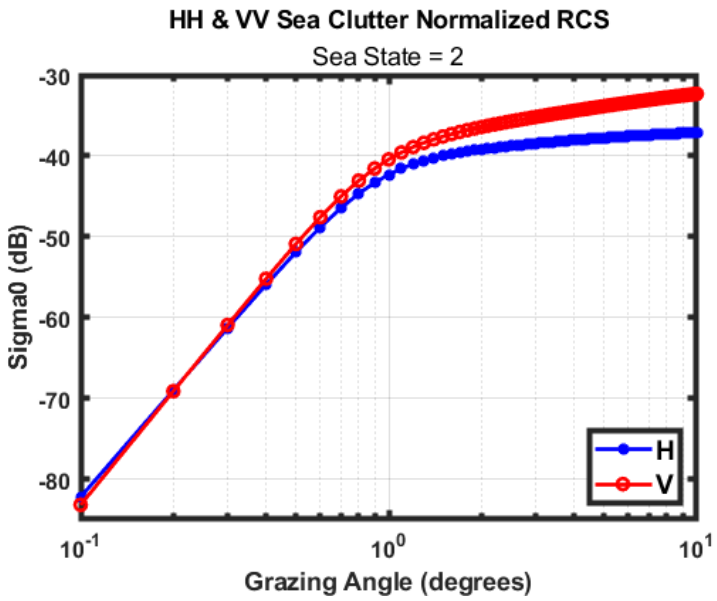

Figure 2.8. HH and VV sea clutter normalized RCS at 10 GHz as a function of grazing angle from the GIT model for sea state 2.

As can be seen in Figure 2.8, horizontally polarized waves have less clutter than vertically polarized ones for $0.2^\circ - 10^\circ$ grazing angles. However, in the range of $0.1^\circ - 0.2^\circ$ grazing angle, horizontally polarized waves have more clutter than vertically polarized ones.

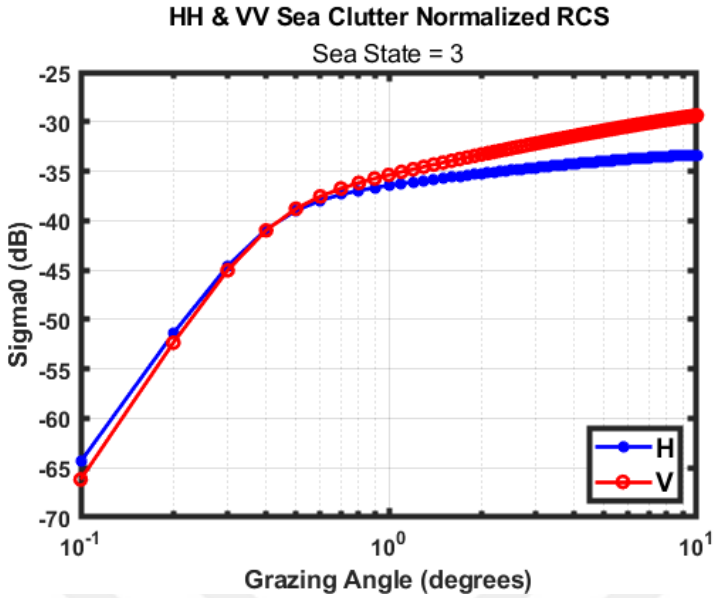

Figure 2.9. HH and VV sea clutter normalized RCS at 10 GHz as a function of grazing angle from the GIT model for sea state 3.

In Figure 2.9, less clutter is calculated for $0.4^{\circ} - 10^{\circ}$ grazing angles when horizontally polarized waves are used. In the $0.1^{\circ} - 0.4^{\circ}$ grazing angle range, vertically polarized waves have less clutter.

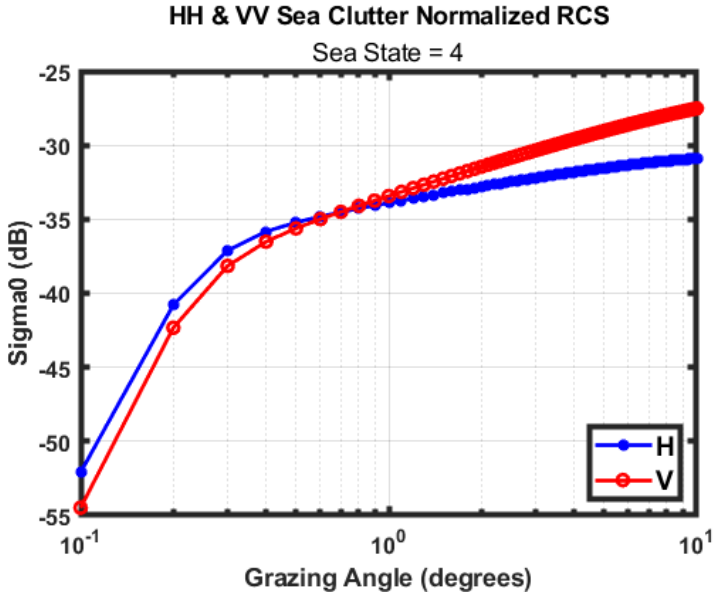

Figure 2.10. HH and VV sea clutter normalized RCS at 10 GHz as a function of grazing angle from the GIT model for sea state 4.

In Figure 2.10, σ^0 is calculated for the sea state is 4. For the range of $0.6^{\circ} - 10^{\circ}$, horizontally polarized waves have less clutter than vertically polarized ones. On the other hand, for $0.1^{\circ} -$

0.6° grazing angles, vertically polarized waves have less clutter than horizontally polarized ones.

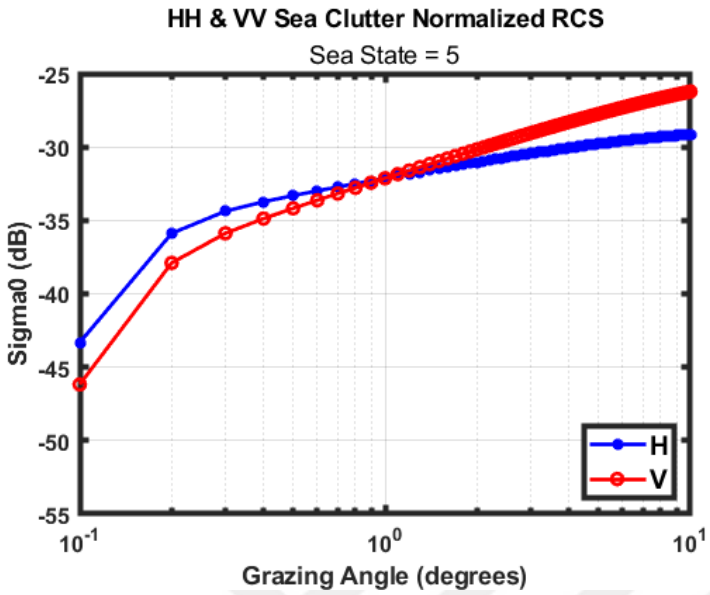

Figure 2.11. HH and VV sea clutter normalized RCS at 10 GHz as a function of grazing angle from the GIT model for sea state 5.

As can be seen in Figure 2.11, horizontally polarized waves have less clutter than vertically polarized ones for $0.9^{\circ} - 10^{\circ}$ grazing angles. However, in the range of $0.1^{\circ} - 0.9^{\circ}$ grazing angle, horizontally polarized waves have more clutter than horizontally polarized ones.

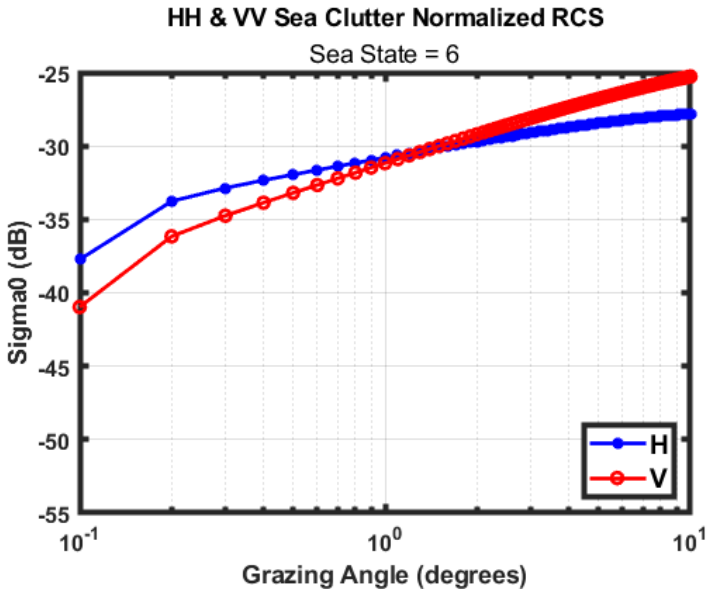

Figure 2.12. HH and VV sea clutter normalized RCS at 10 GHz as a function of grazing angle from the GIT model for sea state 6.

In Figure 2.12, less clutter is calculated for $1.3^{\circ} - 10^{\circ}$ grazing angles when horizontally polarized waves are used. In the $0.1^{\circ} - 1.3^{\circ}$grazing angle range, vertically polarized waves have less clutter.

2.3. Proposed Model

This model was proposed in 2012 by Gregers-Hansen whose IEEE life fellow and Mital whose electronics engineer at Naval Research Laboratory [25]. It has the form:

$$\sigma_{H,V} = c_1 + c_2 * log_{10}(\sin(\alpha)) + \frac{(27.5+c_3*\alpha)*log_{10}(f)}{1+0.95*\alpha} + c_4 * (1+SS)^{\frac{1}{2+0.085*\alpha+0.033*SS}} + c_5 * \alpha^2 \quad (2.11)$$

where α is the grazing angle in degrees, SS is the sea state, f is the radar frequency in GHz, and constants used in the empirical sea clutter model

$$c_{1H} = -73.0,\ c_{1V} = -50.79 \quad (2.12a)$$

$$c_{2H} = 20.78,\ c_{2V} = 25.93 \quad (2.12b)$$

$$c_{3H} = 7.351,\ c_{3V} = 0.7093 \quad (2.12c)$$

$$c_{4H} = 25.65,\ c_{4V} = 21.58 \quad (2.12d)$$

$$c_{5H} = 0.0054,\ c_{5V} = 0.00211 \quad (2.12e)$$

The point of departure for this model is supporting the model to calculate sea clutter using experimental data [26]. The first term of the expression is a constant c_1. It represents the offset of the reflectivity in dB. The second term represents the assumption that sea clutter reflectivity depends on logarithmic grazing angle. The third term which includes c_3, represents the frequency dependence and an empirical correction with grazing angle. The fourth term symbolizes the effect of the sea state on sea clutter and includes an empirical correction with grazing angle. Finally, the fifth term represents the rapid increase in sea clutter reflectivity. While the grazing angle comes close to vertical incidence, reflectivity increases proportional to the square of the grazing angle. Using the above expression and constants, normalized sea clutters are calculated for 6 sea states and $0.1 - 10^{\circ}$ grazing angles. Results are given in Figures 2.13 – Figure 2.18. In Figure 2.13, σ^0 is calculated for

sea state 1. For the whole calculation range, i.e., $0.1 - 10^{\circ}$, horizontally polarized waves have less clutter than vertically polarized ones.

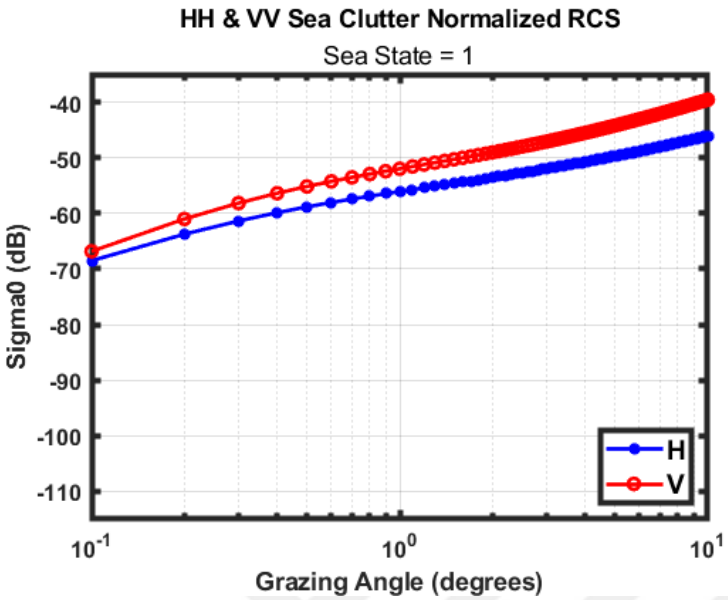

Figure 2.13. HH and VV sea clutter normalized RCS at 10 GHz as a function of grazing angle from the Proposed model for sea state 1.

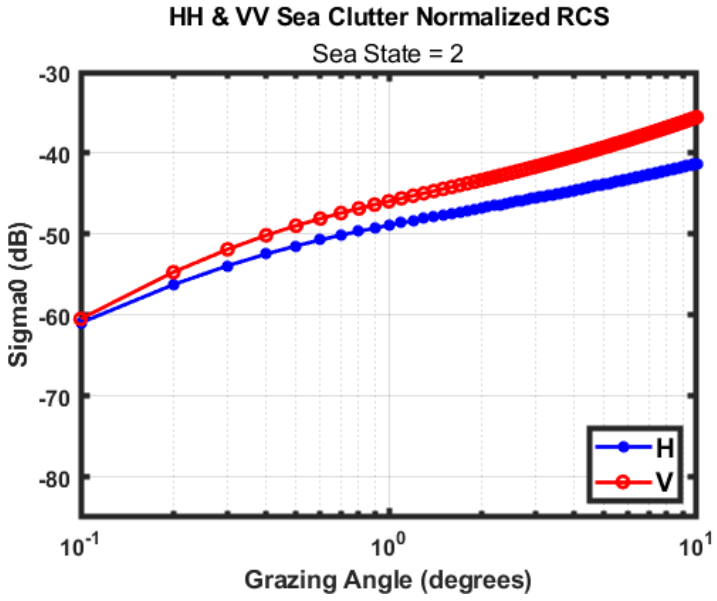

Figure 2.14. HH and VV sea clutter normalized RCS at 10 GHz as a function of grazing angle from the Proposed model for sea state 2.

As can be seen in Figure 2.14, horizontally polarized waves have less clutter than vertically polarized ones for $0.1^{\circ} - 10^{\circ}$ grazing angles.

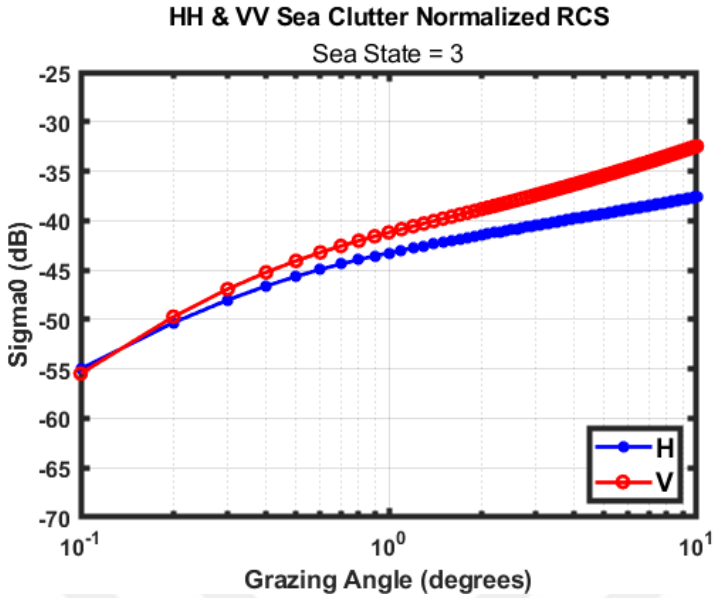

Figure 2.15. HH and VV sea clutter normalized RCS at 10 GHz as a function of grazing angle from the Proposed model for sea state 3.

In Figure 2.15, less clutter is calculated for $0.12^{\circ} - 10^{\circ}$ grazing angles when horizontally polarized waves are used. In the $0.1^{\circ} - 0.12^{\circ}$ grazing angle range, vertically polarized waves have less clutter.

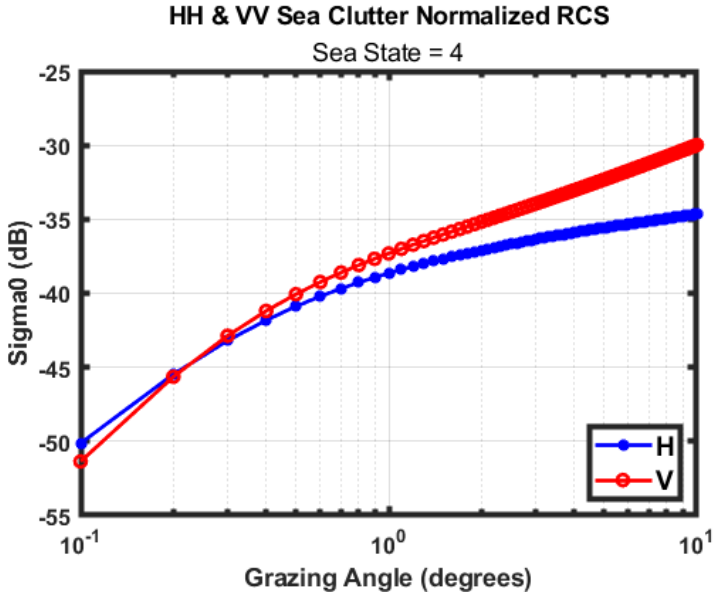

Figure 2.16. HH and VV sea clutter normalized RCS at 10 GHz as a function of grazing angle from the Proposed model for sea state 4.

In Figure 2.16, σ^0 is calculated for sea state 4. For the range of $0.2^{\circ} - 10^{\circ}$, horizontally polarized waves have less clutter than vertically polarized ones. On the other hand, for the

range of $0.1^{\circ} - 0.2^{\circ}$, vertically polarized waves have less clutter than horizontally polarized ones.

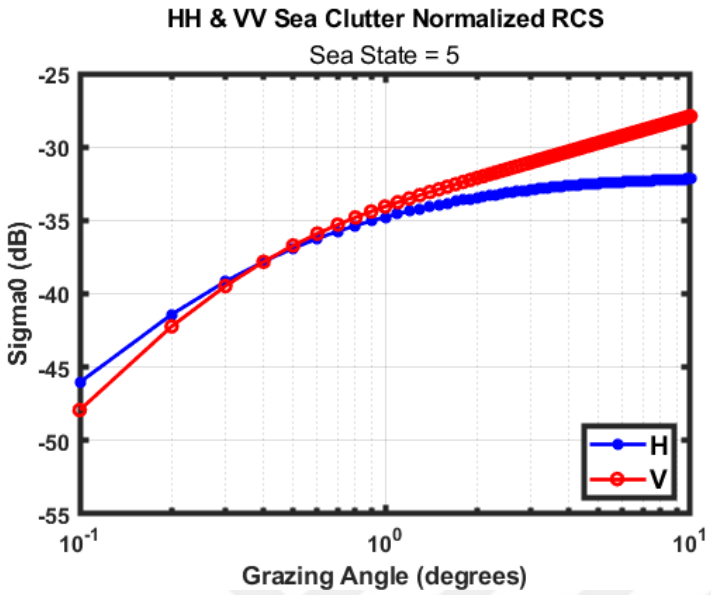

Figure 2.17. HH and VV sea clutter normalized RCS at 10 GHz as a function of grazing angle from the Proposed model for sea state 5.

As can be seen in Figure 2.17, horizontally polarized waves have less clutter than vertically polarized ones for $0.4^{\circ} - 10^{\circ}$ grazing angles. Moreover, horizontally polarized waves have more clutter than vertically polarized ones for $0.1^{\circ} - 0.4^{\circ}$ grazing angles.

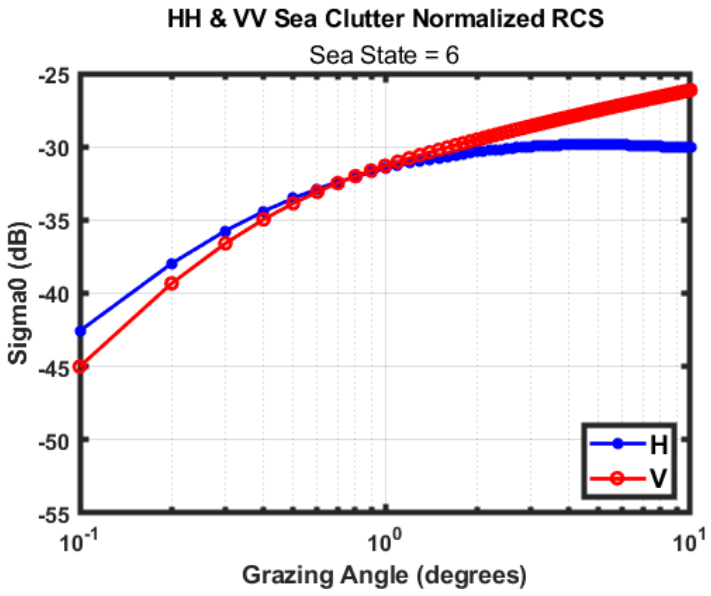

Figure 2.18. HH and VV sea clutter normalized RCS at 10 GHz as a function of grazing angle from the Proposed model for sea state 6.

In Figure 2.18, less clutter is calculated for $0.6^\circ - 10^\circ$ grazing angles when horizontally polarized waves are used. In the $0.1^\circ - 0.6^\circ$ grazing angle range, vertically polarized waves have less clutter.

2.4. NRL Model

This model is also empirical. It is valid for 500 MHz – 35 GHz, and grazing angles for $0.1^\circ - 60^\circ$ [27].

Expression of the model:

$$\sigma^0_{HH,VV} = c_1 + c_2 * log_{10}\left(\sin\left(\Phi_{gr}\right)\right) + \frac{(c_3 + c_4 * \Phi_{gr}) * log_{10}(f)}{1 + c_5 * \Phi_{gr} + c_6 * s} + c_7 * (1 + s)^{\frac{1}{2 + c_8 * \Phi_{gr} + c_9 * s}} \tag{2.13}$$

The constants of the model

$$c_{1H} = -72.76,\ c_{1V} = -48.56 \tag{2.14a}$$

$$c_{2H} = 21.11,\ c_{2V} = 26.30 \tag{2.14b}$$

$$c_{3H} = 24.78,\ c_{3V} = 29.05 \tag{2.14c}$$

$$c_{4H} = 4.917,\ c_{4V} = -0.5183 \tag{2.14d}$$

$$c_{5H} = 0.6216,\ c_{5V} = 1.057 \tag{2.14e}$$

$$c_{6H} = -0.02949,\ c_{6V} = 0.04839 \tag{2.14f}$$

$$c_{7H} = 26.19,\ c_{7V} = 21.37 \tag{2.14g}$$

$$c_{8H} = 0.09345,\ c_{8V} = 0.07466 \tag{2.14h}$$

$$c_{9H} = 0.05031,\ c_{9V} = 0.04623 \tag{2.14i}$$

Using the above expressions and constants, normalized sea clutters are calculated for 6 sea states and $0.1^\circ - 10^\circ$ grazing angles. Results are given in Figures 2.19 – Figure 2.24.

In Figure 2.19, σ^0 is calculated for sea state 1. For the whole calculation range, i.e., $0.1^\circ - 10^\circ$, horizontally polarized waves have less clutter than vertically polarized ones.

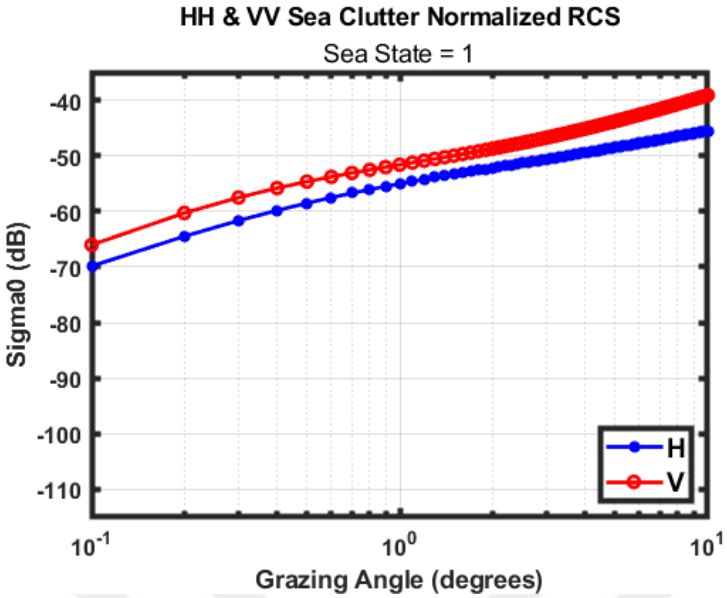

Figure 2.19. HH and VV sea clutter normalized RCS at 10 GHz as a function of grazing angle from the NRL model for sea state 1.

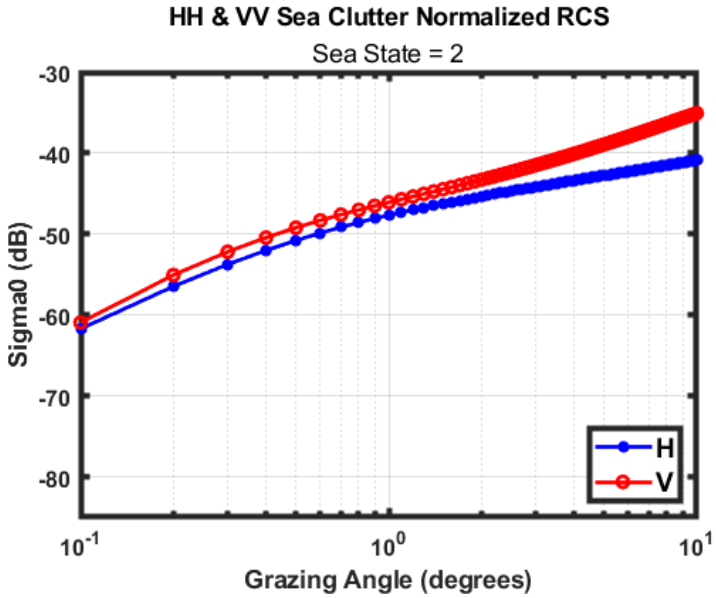

Figure 2.20. HH and VV sea clutter normalized RCS at 10 GHz as a function of grazing angle from the NRL model for sea state 2.

As can be seen in Figure 2.20, for the whole calculation range, i.e., $0.1^{\circ} - 10^{\circ}$, horizontally polarized waves have less clutter than vertically polarized ones.

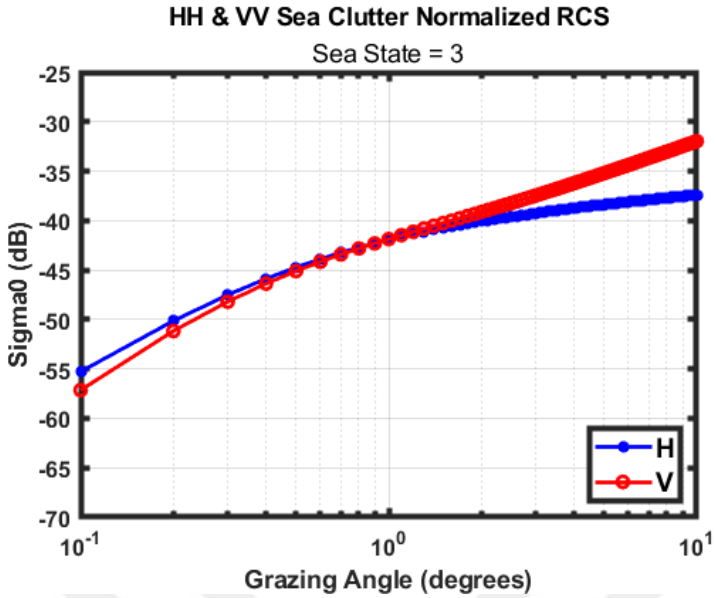

Figure 2.21. HH and VV sea clutter normalized RCS at 10 GHz as a function of grazing angle from the NRL model for sea state 3.

In Figure 2.21, less clutter is calculated for $0.9^{\circ} - 10^{\circ}$ grazing angles when horizontally polarized waves are used. In the $0.1^{\circ} - 0.9^{\circ}$ grazing angle range, vertically polarized waves have less clutter.

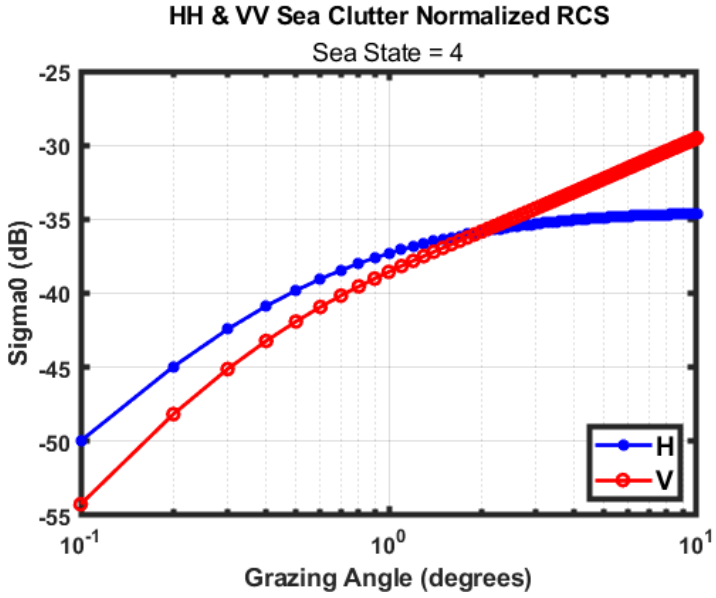

Figure 2.22. HH and VV sea clutter normalized RCS at 10 GHz as a function of grazing angle from the NRL model for sea state 4.

In Figure 2.22, σ^0 is calculated for sea state 4. For the range of $1^{\circ} - 10^{\circ}$ grazing angles, horizontally polarized waves have less clutter than vertically polarized ones. Also,

horizontally polarized waves have more clutter than vertically polarized ones for the range of $0.1^{\circ} - 1^{\circ}$ grazing angles.

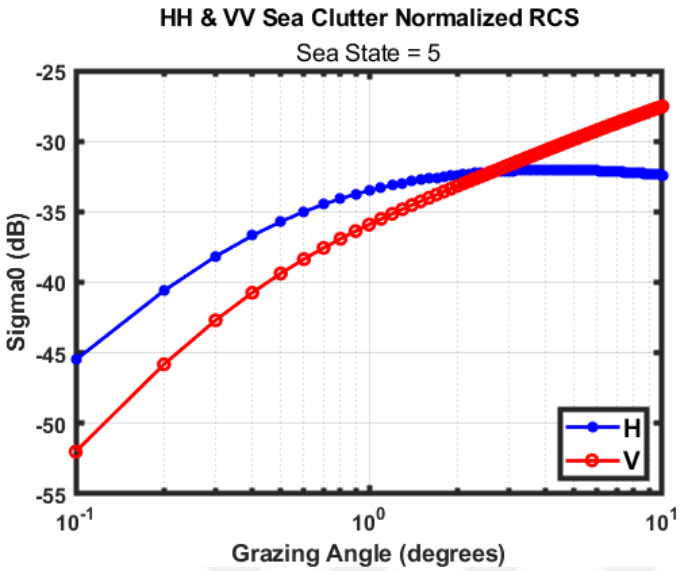

Figure 2.23. HH and VV sea clutter normalized RCS at 10 GHz as a function of grazing angle from the NRL model for sea state 5.

As can be understood from Figure 2.23 for the range of $2.5^{\circ} - 10^{\circ}$ grazing angles, horizontally polarized waves have less clutter than vertically polarized ones. Also, horizontally polarized waves have more clutter than vertically polarized ones for the range of $0.1^{\circ} - 2.5^{\circ}$ grazing angles.

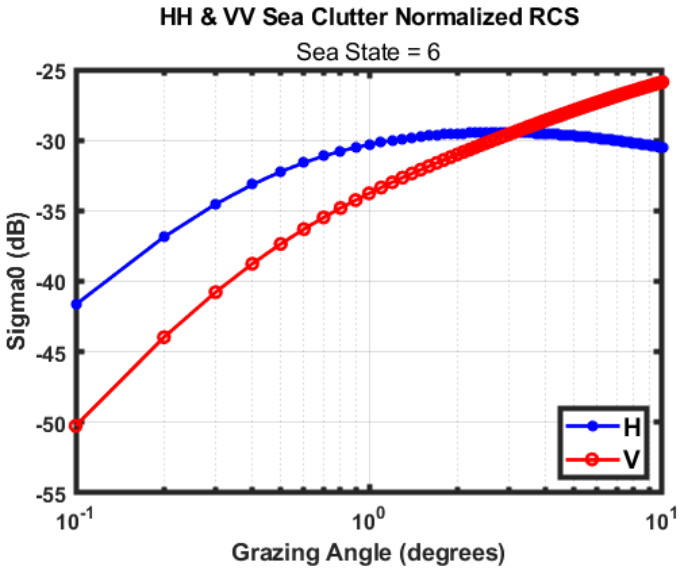

Figure 2.24. HH and VV sea clutter normalized RCS at 10 GHz as a function of grazing angle from the NRL model for sea state 6.

In Figure 2.24, horizontally polarized waves have less clutter than vertically polarized ones in the range of $3.1^{\circ} - 10^{\circ}$ grazing angles. On the other hand, horizontally polarized waves have more clutter than vertically polarized ones in the range of $0.1^{\circ} - 3.1^{\circ}$ grazing angles.

The average of the horizontal polarization wave of the four models and sea state 6 is $-30.38\ dB$ at the 10° grazing angle. Moreover, the average of vertical polarization is $-26.32\ dB$. This 4.06 dB difference thanks to using horizontally polarized waves provides an increase in the maximum radar range of 1.37 times. Range difference is calculated by using the following equation [28]:

$$R_0 = \left(\frac{P_t * G^2 * \lambda^2 * \sigma^0 * \Delta R * \Theta_3}{(4*\pi)^3 * P_r * L_s * \cos(\delta)}\right)^{1/3} \quad (2.15)$$

where,

R_0: The distance between the antenna and the surface (m)

P_t: Power transmitted from the transmitter (Watts)

G: Antenna power gain

λ: Wavelength (m)

ΔR: Range resolution (m)

Θ_3: 3 dB azimuth beamwidth (radian)

P_r: Power received at the receiver (Watts)

L_s: System loss factor

δ: Grazing angle (degree).

The average of the horizontal polarization wave of the four models and sea state 5 is $-32.17\ dB$ at the 10° grazing angle. Moreover, the average of the vertical polarization is $-27.66\ dB$. This 4.51 dB difference provides an increase in the maximum radar range of 1.41 times.

The average of the horizontal polarization wave of the four models and sea state 4 is $-34.46\ dB$ at the 10° grazing angle. Moreover, the average of the vertical polarization is $-29.50\ dB$. This 4.96 dB difference provides an increase in the maximum radar range of 1.46 times.

The average of the horizontal polarization wave of the four models and sea state 3 is $-37.08\ dB$ at the 10° grazing angle. Moreover, the average vertical polarization is

$-31.7\ dB$. This $5.38\ dB$ difference provides an increase in the maximum radar range of 1.51 times.

The average of the horizontal polarization wave of the four models and sea state 2 is $-40.46\ dB$ at the 10° grazing angle. Moreover, the average of the vertical polarization is $-36.18\ dB$. This $4.28\ dB$ difference provides an increase in the maximum radar range of 1.39 times.

The average of the horizontal polarization wave of the four models and sea state 1 is $-46.72\ dB$ at the 10° grazing angle. Moreover, the average of the vertical polarization is $-40.05\ dB$. This $6.67\ dB$ difference provides an increase in the maximum radar range of 1.67 times.

Range difference increases while the average increases as the formula indicates. The average of the horizontal and vertical polarization waves of the four models for sea clutter is shown in Table 2.2.

Table 2.2. Sea clutter for four models and $0.1^{\circ} - 10^{\circ}$ grazing angles (in dB)

	Model	RRE		GIT		Proposed		NRL	
	Pol.	H	V	H	V	H	V	H	V
Grazing Angle	Sea State								
0.1°	1	-73.0	-66.5	-113.51	-113.15	-68.51	-66.82	-69.84	-66.02
0.1°	2	-63.5	-57.5	-82.23	-83.2	-60.97	-60.48	-61.71	-60.92
0.1°	3	-54.5	-52.5	-64.39	-66.18	-55.47	-55.01	-55.28	-57.15
0.1°	4	-49.5	-49.5	-52.09	-54.48	-51.36	-50.12	-49.98	-54.25
0.1°	5	-44.0	-45.5	-43.32	-46.18	-46.04	-47.92	-45.5	-52.0
0.1°	6	-39.0	-42.5	-37.73	-40.97	-42.57	-45.0	-41.65	-50.25
1°	1	-52.0	-51.5	-42.32	-40.43	-56.08	-51.98	-55.03	-51.62
1°	2	-46.0	-45.5	-69.63	-66.42	-48.91	-45.95	-47.66	-46.07
1°	3	-42.0	-41.0	-36.44	-35.38	-43.27	-41.2	-41.93	-41.87
1°	4	-39.0	-38.5	-33.9	-33.43	-38.65	-37.31	-37.31	-38.56
1°	5	-37.0	-36.0	-32.14	-32.13	-34.78	-34.06	-33.5	-35.91
1°	6	-35.5	-34.5	-30.8	-31.17	-31.5	-31.3	-30.3	-33.77
10°	1	-50.99	-43.3	-44.38	-38.25	-46.02	-39.55	-45.48	-39.11
10°	2	-42.61	-36.0	-37.11	-32.31	-41.25	-35.55	-40.87	-35.04
10°	3	-39.97	-33.0	-33.34	-29.36	-37.6	-32.47	-37.39	-31.97
10°	4	-37.65	-31.0	-30.9	-27.51	-34.64	-29.98	-34.64	-29.52
10°	5	-34.97	-29.0	-29.14	-26.22	-32.17	-27.9	-32.39	-27.53
10°	6	-33.13	-28.0	-27.81	-25.26	-30.07	-26.14	-30.52	-25.87

2.5. Comparison of Models

In this part of the thesis, four models are used to calculate sea clutter are compared in each sea state. In Figures 2.25 – Figure 2.30, models are compared in terms of horizontal polarization, and in Figures 2.31 – Figure 2.36, models are compared in terms of vertical one.

It can be understood that from Figure 2.25 and Figure 2.26 three of the models give similar results. On the other hand, the GIT model gives 40 dB less clutter at the 0.1° grazing angle than the RRE, Proposed, and NRL models.

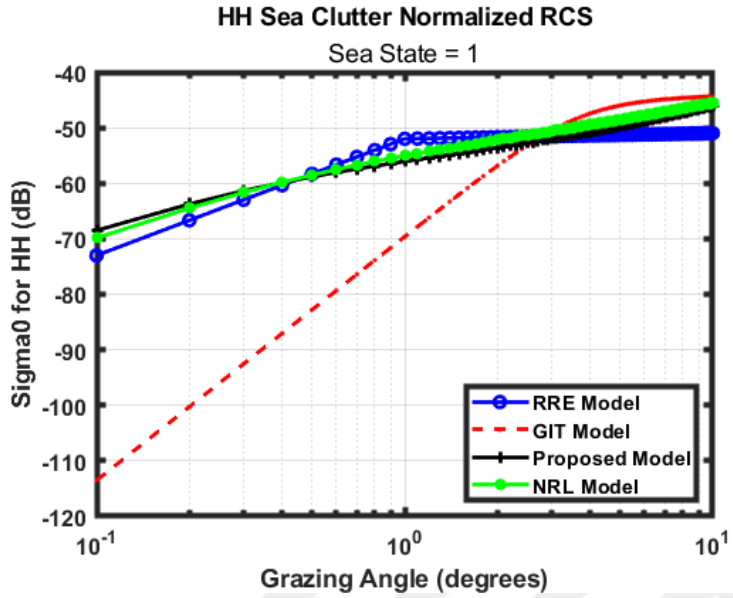

Figure 2.25. HH sea clutter normalized RCS at 10 GHz as a function of grazing angle from all models for sea state 1.

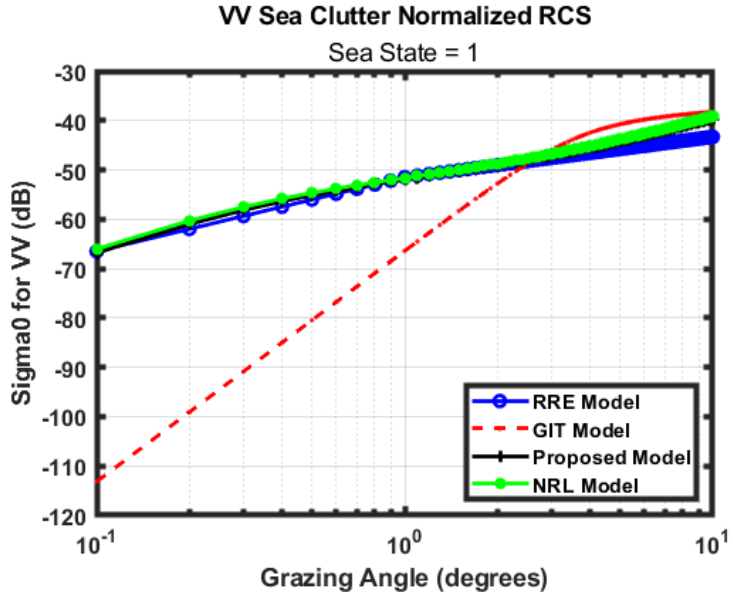

Figure 2.26. HH sea clutter normalized RCS at 10 GHz as a function of grazing angle from all models for sea state 2.

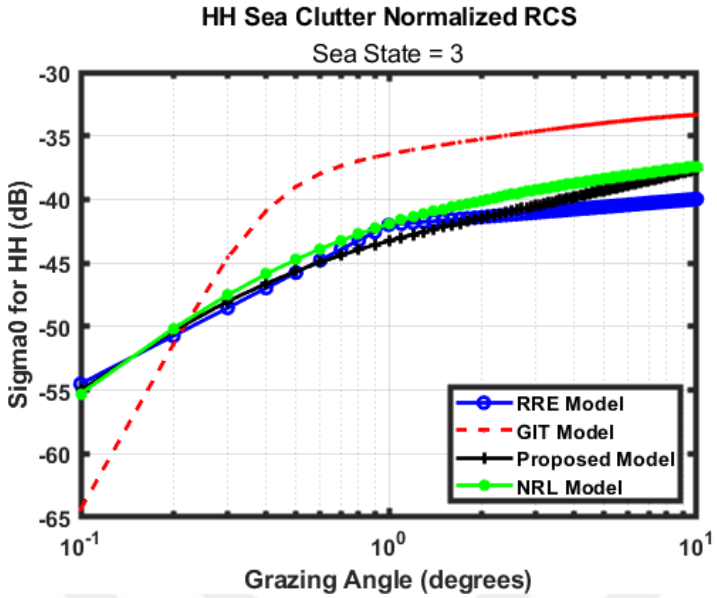

Figure 2.27. HH sea clutter normalized RCS at 10 GHz as a function of grazing angle from all models for sea state 3.

In Figure 2.27, the GIT model gives 10 dB less clutter at the 0.1° grazing angle than the other three models. After the 0.2° grazing angle, it gives the higher clutter.

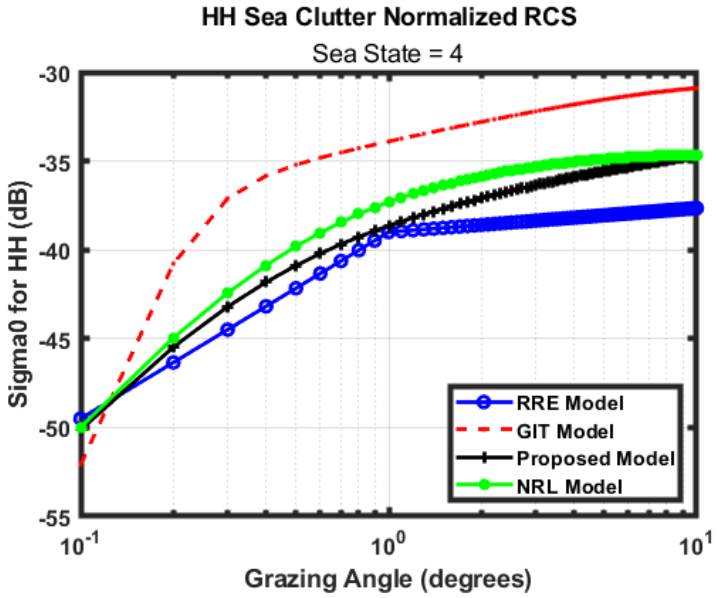

Figure 2.28. HH sea clutter normalized RCS at 10 GHz as a function of grazing angle from all models for sea state 4.

In Figure 2.28, σ^0 is calculated for sea state 4. All of the models give the same result at the 0.1° grazing angle. For the whole range of grazing angle, i.e., $0.1^{\circ} - 10^{\circ}$, Proposed and NRL

models give the nearest results. On the other hand, the RRE model gives 3 dB less clutter, and the GIT model gives 4 dB more clutter than these two.

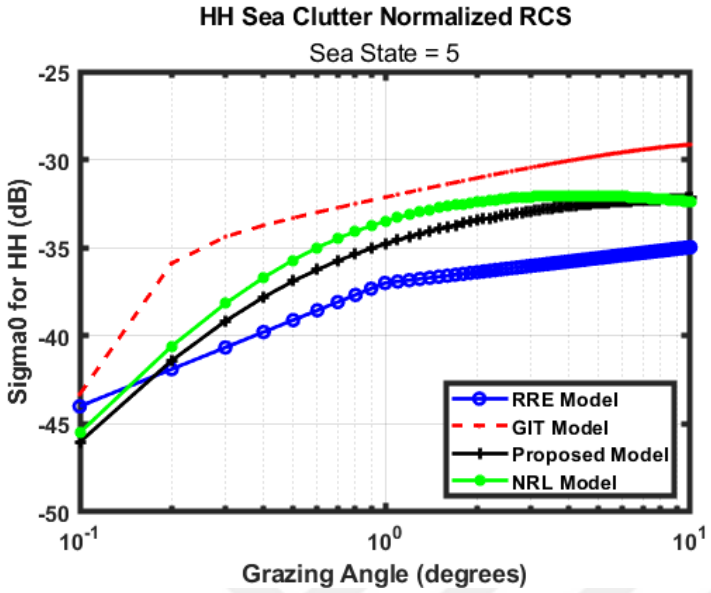

Figure 2.29. HH sea clutter normalized RCS at 10 GHz as a function of grazing angle from all models for sea state 5.

Figure 2.29 and Figure 2.30 show that the Proposed and NRL models give similar results for the whole calculation range, i.e. $0.1^{\circ} - 10^{\circ}$ grazing angle. While the RRE model has lower clutter, the GIT model has more clutter than them at the 10° grazing angle.

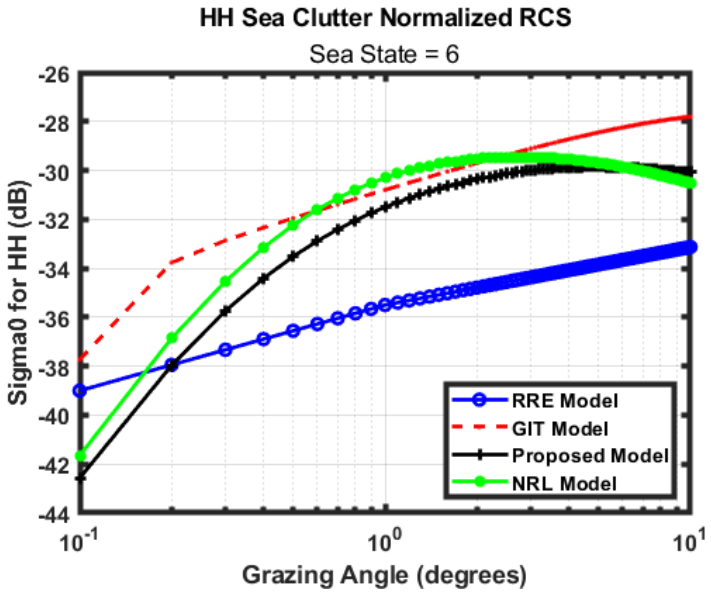

Figure 2.30. HH sea clutter normalized RCS at 10 GHz as a function of grazing angle from all models for sea state 6.

In Figure 2.31, σ^0 is calculated for sea state 1. Three of the models give similar results. On the other hand, the GIT model gives 40 dB less clutter at the 0.1° grazing angle and the equal result with the NRL model at the 10° grazing angle.

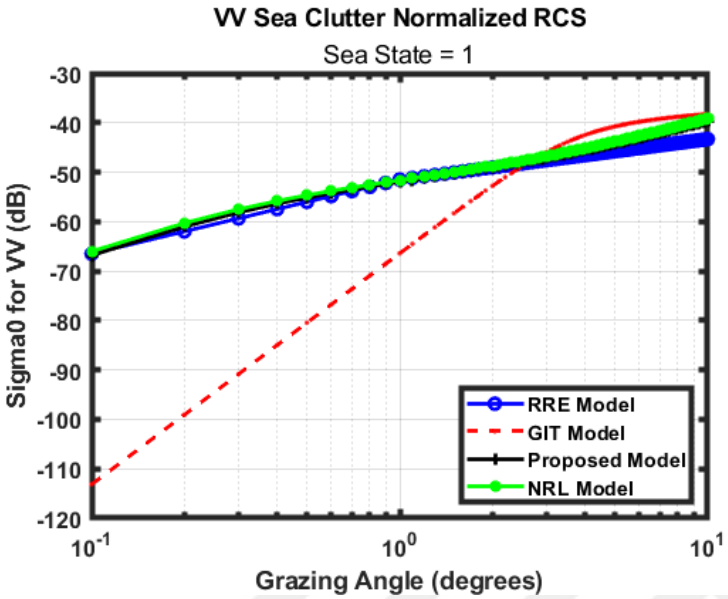

Figure 2.31. VV sea clutter normalized RCS at 10 GHz as a function of grazing angle from all models for sea state 1.

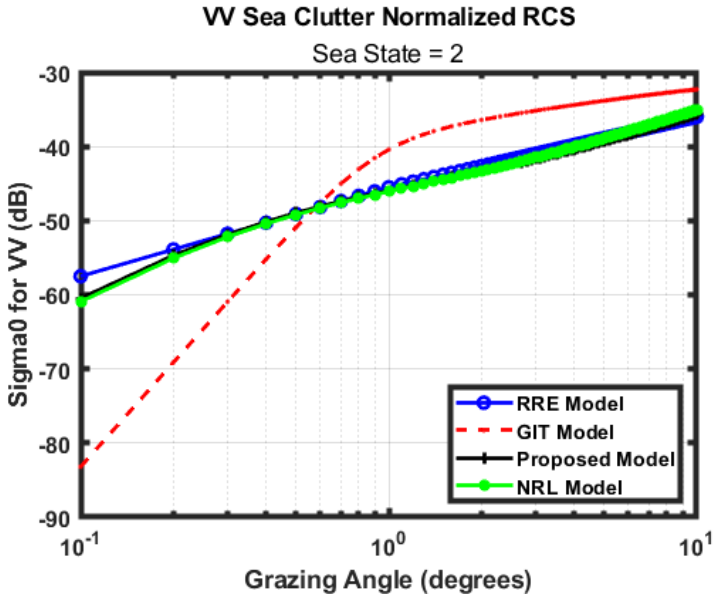

Figure 2.32. VV sea clutter normalized RCS at 10 GHz as a function of grazing angle from all models for sea state 2.

In Figure 2.32 and Figure 2.33, while three of models give the similar results GIT model gives less clutter than the other three models 20 dB and 10 dB, respectively at 0.1°. On the other hand, it gives more clutter at 10°.

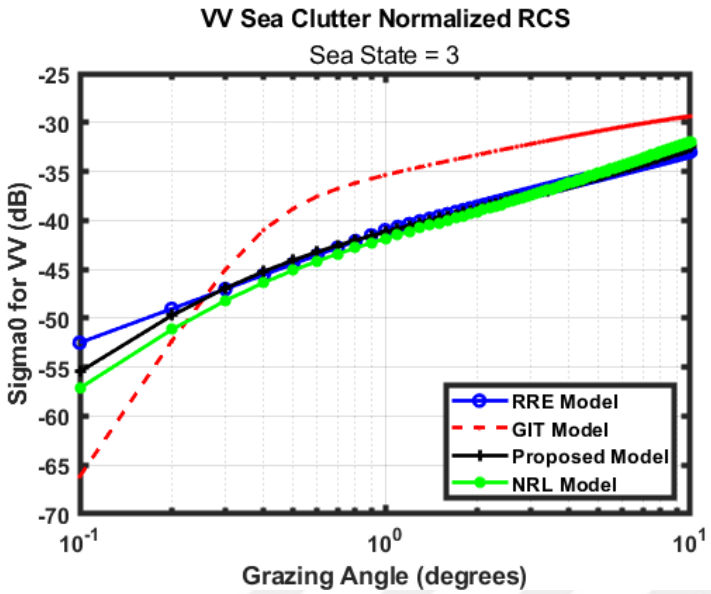

Figure 2.33. VV sea clutter normalized RCS at 10 GHz as a function of grazing angle from all models for sea state 3.

In Figure 2.34, three of the models give similar results for the whole grazing angle range i.e., $0.1^{\circ} - 10^{\circ}$.

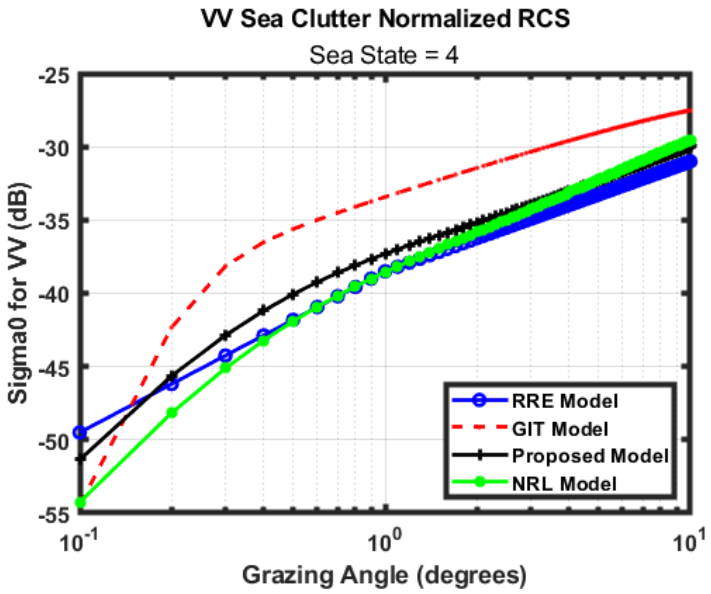

Figure 2.34. VV sea clutter normalized RCS at 10 GHz as a function of grazing angle from all models for sea state 4.

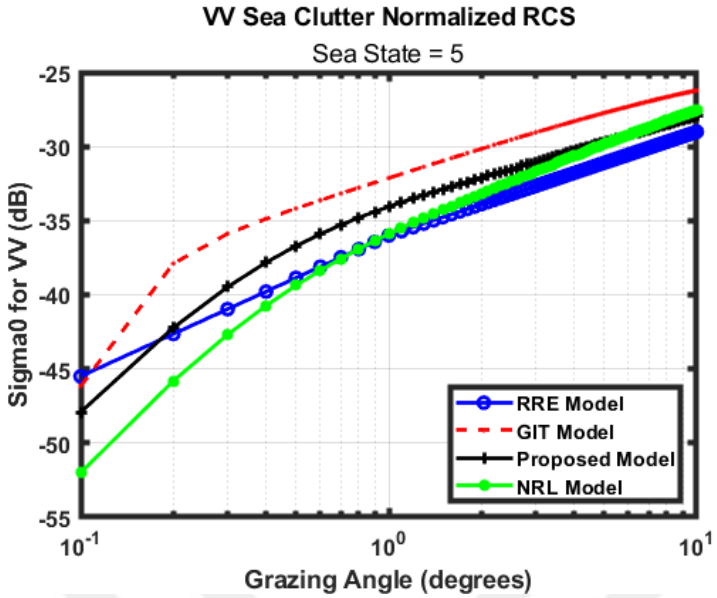

Figure 2.35. VV sea clutter normalized RCS at 10 GHz as a function of grazing angle from all models for sea state 5.

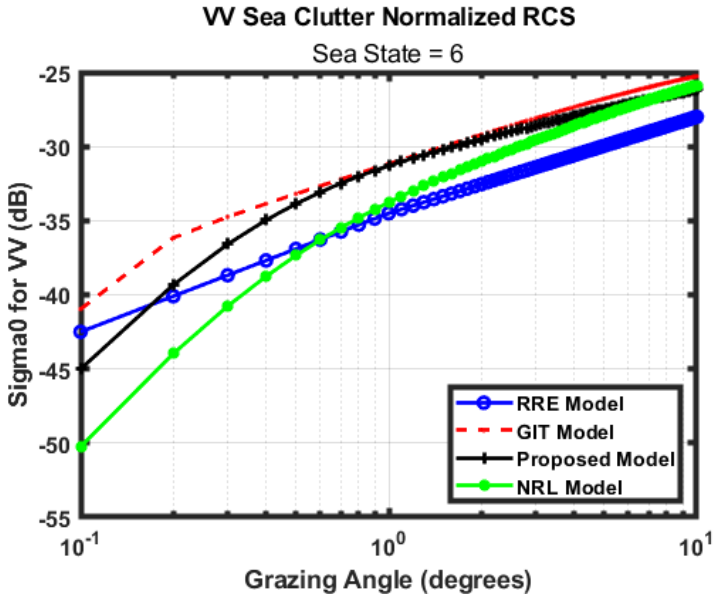

Figure 2.36. VV sea clutter normalized RCS at 10 GHz as a function of grazing angle from all models for sea state 6.

As can be seen in Figure 2.35 and Figure 2.36 four models give similar sea clutter results at the 10° grazing angle for sea states 5 and 6, respectively.

2.6. Comparison of Sea States

In this part of the thesis, four models that are used to calculate sea clutter are compared for each sea state. In Figure 2.37 – Figure 2.40, sea clutter is calculated for horizontal polarization, and in Figure 2.41 – Figure 2.44, it is calculated for vertical one.

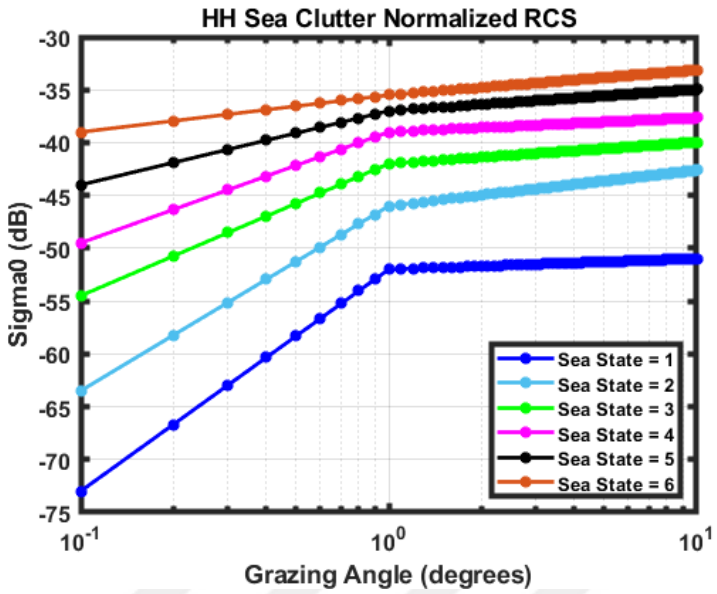

Figure 2.37. HH sea clutter normalized RCS at 10 GHz as a function of grazing angle from the RRE model for all sea states.

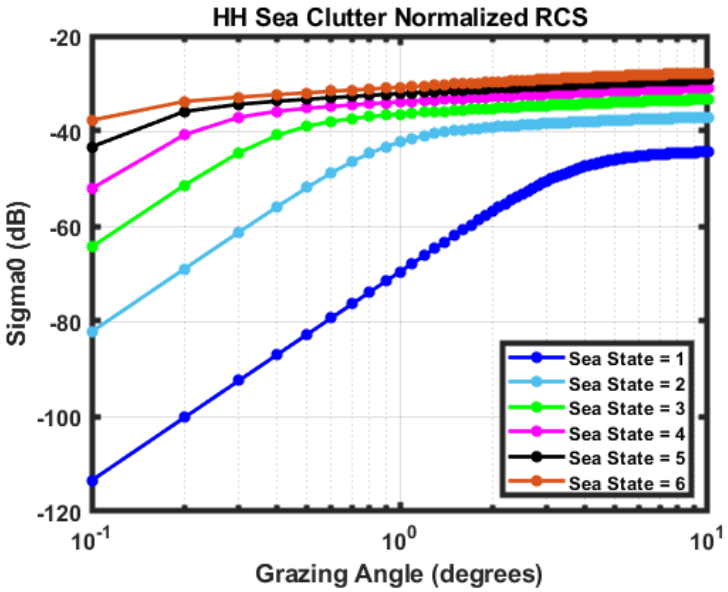

Figure 2.38. HH sea clutter normalized RCS at 10 GHz as a function of grazing angle from the GIT model for all sea states.

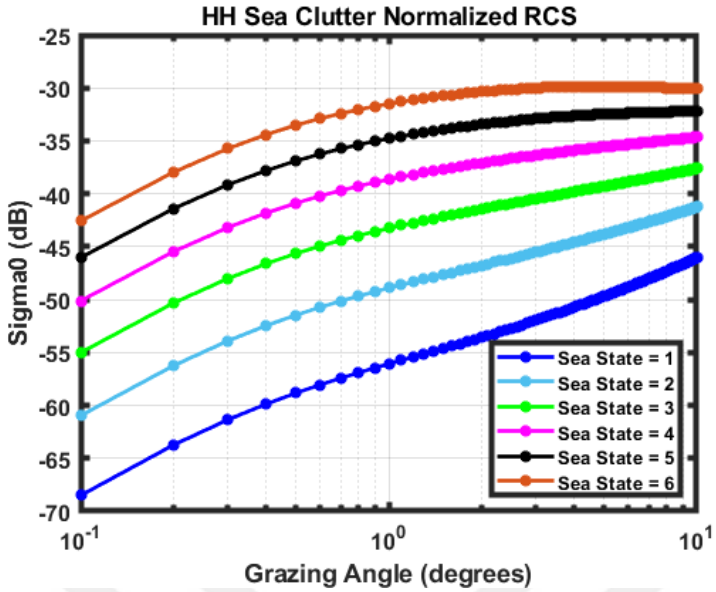

Figure 2.39. HH sea clutter normalized RCS at 10 GHz as a function of grazing angle from the Proposed model for all sea states.

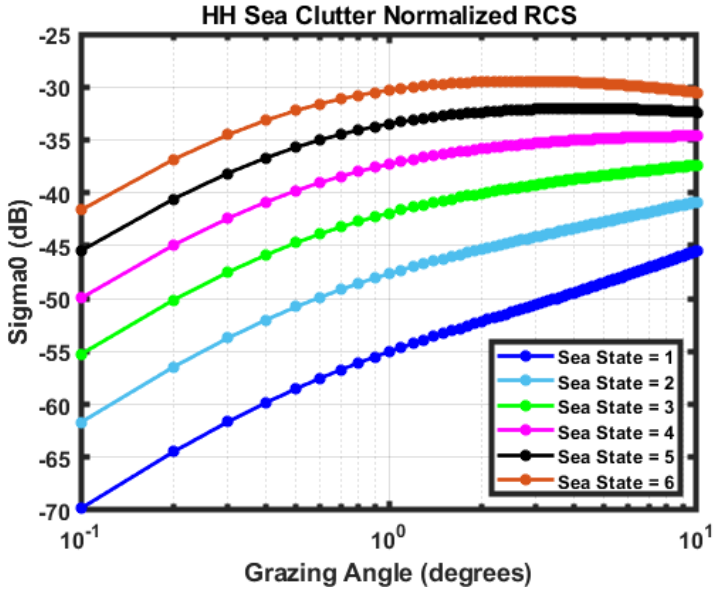

Figure 2.40. HH sea clutter normalized RCS at 10 GHz as a function of grazing angle from the NRL model for all sea states.

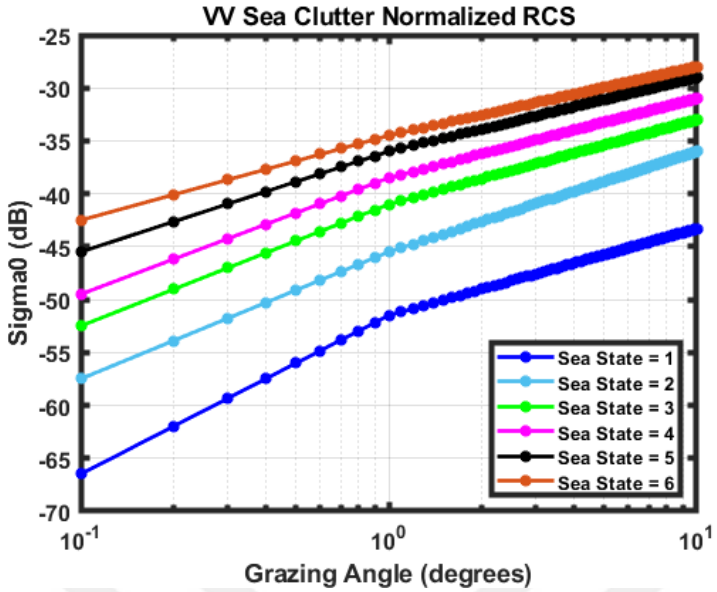

Figure 2.41. VV sea clutter normalized RCS at 10 GHz as a function of grazing angle from the RRE model for all sea states.

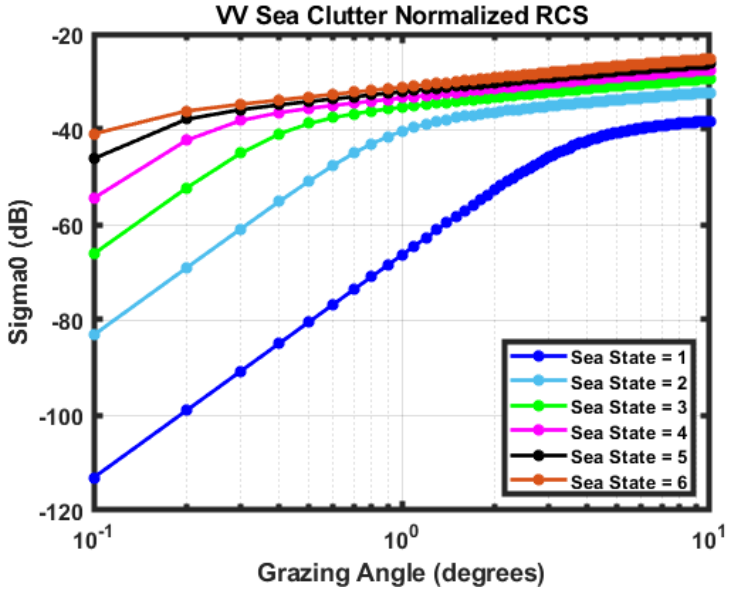

Figure 2.42. VV sea clutter normalized RCS at 10 GHz as a function of grazing angle from the GIT model for all sea states.

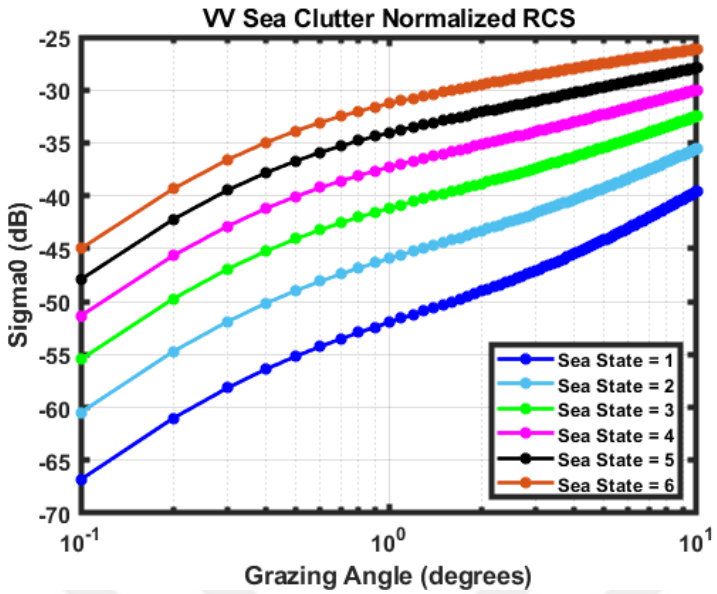

Figure 2.43. VV sea clutter normalized RCS at 10 GHz as a function of grazing angle from the Proposed model for all sea states.

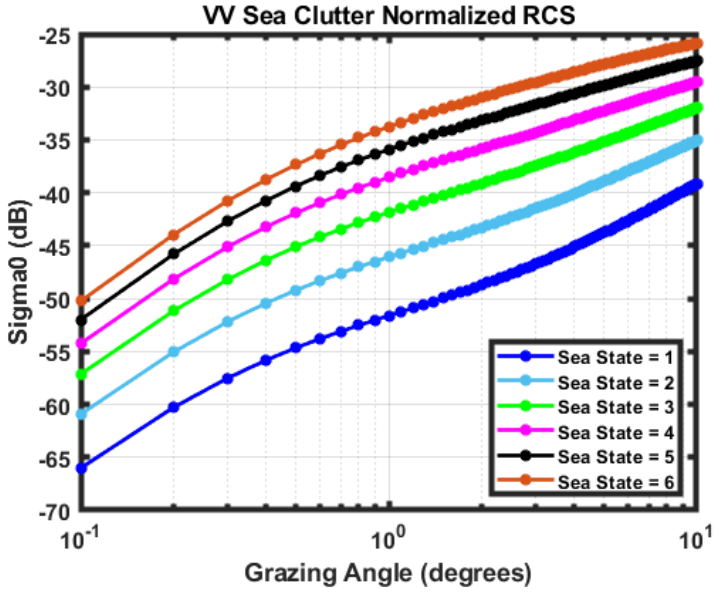

Figure 2.44. VV sea clutter normalized RCS at 10 GHz as a function of grazing angle from the NRL model for all sea states.

The conclusion is common for all of the comparisons: The sea clutter and sea state are proportional, i.e. as the sea state increases, the sea clutter increases.

3. LAND CLUTTER

There are different models to calculate land clutter such as Barton, APL, Billingesley, GIT, Morchin, Nathanson, and Ulaby & Dobson. Ulaby & Dobson's model is examined since it calculated the land clutter according to polarization.

3.1. Ulaby and Dobson Model

It is a semi-empirical model for frequencies 1 - 18 GHz and $0-60^{\circ}$ grazing angles and different land types such as soil and rock surfaces, grasses, shrubs, short vegetation, road surfaces, dry snow, and wet snow [29]. These categories will be examined, respectively. Expression of the model:

$$\sigma^0_{HH,VV} = P_1 + P_2 * \exp(-P_3 * \theta) + P_4 * \cos(P_5 * \theta + P_6) \quad (3.1)$$

where θ is the incidence angle in radians and it is related to the grazing angle with the equation of $\theta = \frac{\pi}{2} - \Phi_{gr}$. Also, P_1, P_2, P_3, P_4, P_5, and P_6 are the parameters that are dependent on the land type and polarization.

3.1.1. Soil and rock surfaces

These surfaces are sparsely vegetated.

Parameters of the model for X-band:

$$P_{1H} = 4.337, P_{1V} = -42.553 \quad (3.2a)$$

$$P_{2H} = 6.666, P_{2V} = 48.823 \quad (3.2b)$$

$$P_{3H} = -0.107, P_{3V} = 0.722 \quad (3.2c)$$

$$P_{4H} = -29.709, P_{4V} = 5.808 \quad (3.2d)$$

$$P_{5H} = 0.863, P_{5V} = 3.000 \quad (3.2e)$$

$$P_{6H} = -1.365, P_{6V} = -3.142 \quad (3.2f)$$

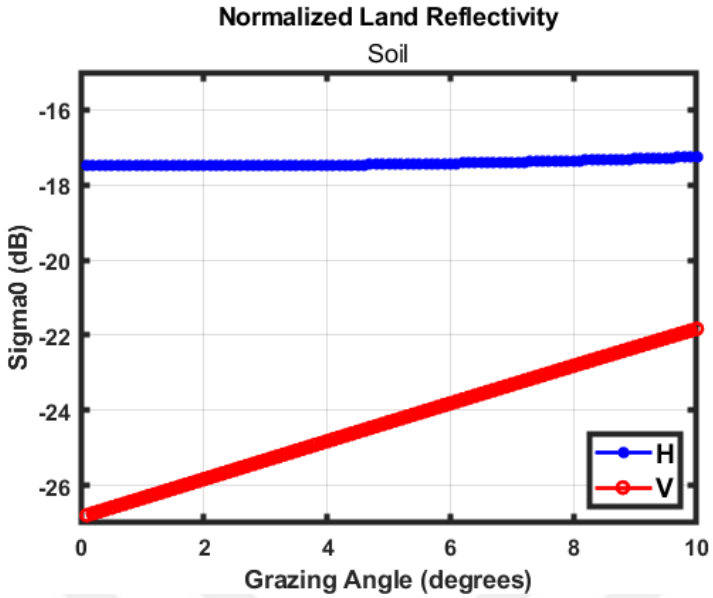

Figure 3.1. Land clutter normalized RCS at 10 GHz as a function of grazing angle from the Ulaby and Dobson model for soil.

Figure 3.1 shows that horizontally polarized waves have more reflectivity than vertically polarized waves for $0.1^{\circ} - 10^{\circ}$ grazing angles.

3.1.2. Grasses

Grasses are pasture, hay, and small grains such as barley, oats, rye, and wheat.

Parameters of the model for X-band:

$$P_{1H} = -33.288,\ P_{1V} = -22.177 \tag{3.3a}$$

$$P_{2H} = 32.980,\ P_{2V} = 21.891 \tag{3.3b}$$

$$P_{3H} = 0.510,\ P_{3V} = 1.054 \tag{3.3c}$$

$$P_{4H} = -1.343,\ P_{4V} = -1.916 \tag{3.3d}$$

$$P_{5H} = 4.874,\ P_{5V} = 4.555 \tag{3.3e}$$

$$P_{6H} = -3.142,\ P_{6V} = -2.866 \tag{3.3f}$$

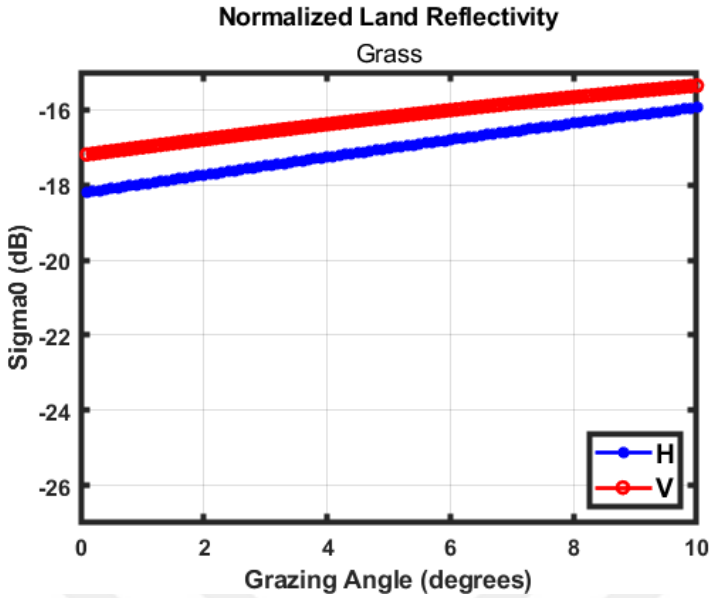

Figure 3.2. Land clutter normalized RCS at 10 GHz as a function of grazing angle from the Ulaby and Dobson model for grass.

Figure 3.2 shows that vertically polarized waves have more reflectivity than horizontally polarized waves for $0.1^{\circ} - 10^{\circ}$ grazing angles.

3.1.3. Shrubs

This land type includes:

- natural herbaceous shrubs,
- large grains such as corn, milo, and sorghum,
- legumes such as beans, peas, and soybeans,
- root crops such as carrots, onions, potatoes, and sugar beets,
- forage crops such as alfalfa,
- canola, and
- cotton.

In terms of growth habits, they are typically bushy. After harvesting, this land type becomes the soil and rock type.

Parameters of the model for X-band:

$$P_{1H} = -99.000, P_{1V} = -99.000 \quad (3.4a)$$

$P_{2H} = 97.280, P_{2V} = 97.682$ (3.4b)

$P_{3H} = 0.107, P_{3V} = 0.113$ (3.4c)

$P_{4H} = -0.538, P_{4V} = -0.779$ (3.4d)

$P_{5H} = 5.000, P_{5V} = 5.000$ (3.4e)

$P_{6H} = -2.688, P_{6V} = -2.076$ (3.4f)

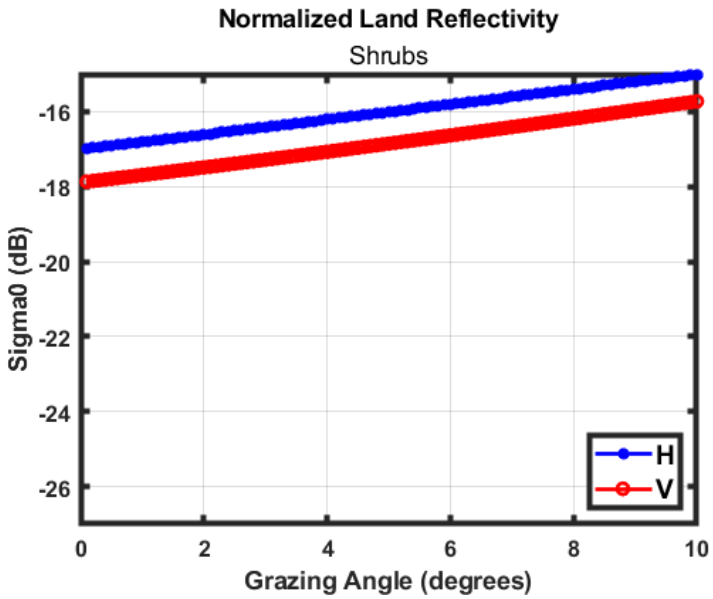

Figure 3.3. Land clutter normalized RCS at 10 GHz as a function of grazing angle from the Ulaby and Dobson model for shrubs.

Figure 3.3 shows that horizontally polarized waves have more reflectivity than vertically polarized waves for $0.1^{\circ} - 10^{\circ}$ grazing angles.

3.1.4. Short vegetation

It is also called a wetland. It includes marshes, swamps, and flooded agricultural land. Hence, this type is highly variable in terms of the amount and nature of biomass and plant geometry.

Parameters of the model for X-band:

$P_{1H} = -99.000, P_{1V} = -99.000$ (3.5a)

$P_{2H} = 97.417, P_{2V} = 97.370$ (3.5b)

$$P_{3H} = 0.114, P_{3V} = 0.119 \quad (3.5c)$$

$$P_{4H} = -0.837, P_{4V} = -1.171 \quad (3.5d)$$

$$P_{5H} = 5.000, P_{5V} = 5.000 \quad (3.5e)$$

$$P_{6H} = -2.984, P_{6V} = -2.728 \quad (3.5f)$$

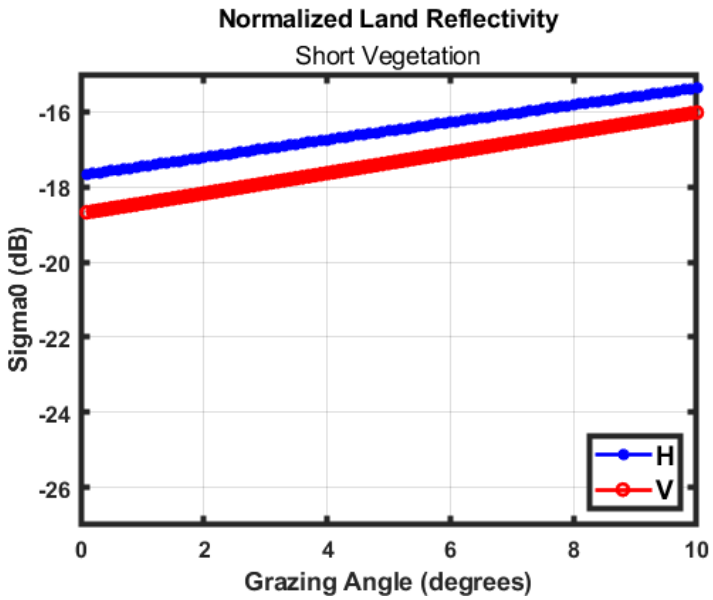

Figure 3.4. Land clutter normalized RCS at 10 GHz as a function of grazing angle from the Ulaby and Dobson model for short vegetation.

Figure 3.4 shows that horizontally polarized waves have more reflectivity than vertically polarized waves for $0.1^{\circ} - 10^{\circ}$ grazing angles.

3.1.5. Road surfaces

Using truck-mounted scatterometers, backscatter data are measured from road surfaces. This land type includes asphalt, concrete, and gravel.

Parameters of the model for X-band:

$$P_{1H} = -94.472, P_{1V} = -38.159 \quad (3.6a)$$

$$P_{2H} = 99.000, P_{2V} = 39.284 \quad (3.6b)$$

$$P_{3H} = 0.892, P_{3V} = 1.598 \quad (3.6c)$$

$$P_{4H} = 30.000, P_{4V} = 30.000 \quad (3.6d)$$

$$P_{5H} = 1.562, P_{5V} = 1.184 \quad (3.6e)$$

$$P_{6H} = -1.918, P_{6V} = -1.178 \quad (3.6f)$$

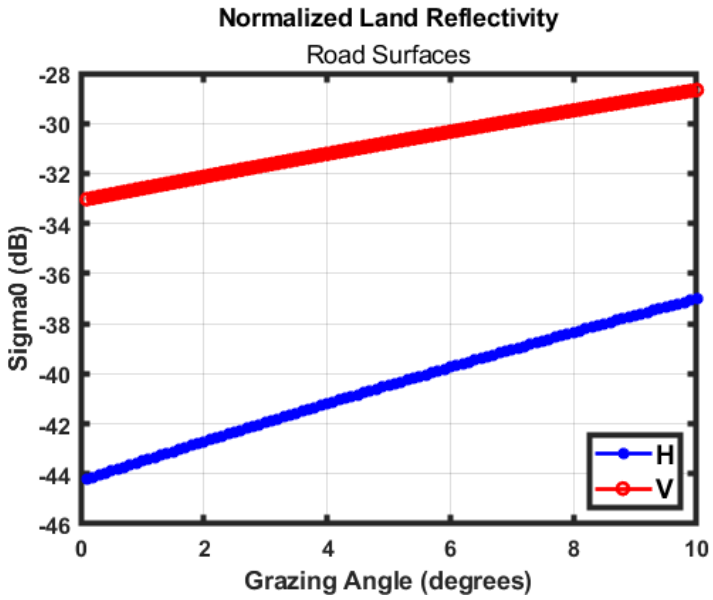

Figure 3.5. Land clutter normalized RCS at 10 GHz as a function of grazing angle from the Ulaby and Dobson model for road surfaces.

Figure 3.5 shows that vertically polarized waves have more reflectivity than horizontally polarized waves for $0.1^{\circ} - 10^{\circ}$ grazing angles.

3.1.6. Dry snow

Snow land type defines the surface that is continuously covered by snow. The only physical property of snow that can be used to subclassify is snow wetness. To classify the snow as dry and wet, the liquid water in snow is used. Dry snow has a liquid water content (LWC) smaller than 1 percent of its volume.

Parameters of the model for X-band:

$$P_{1H} = -13.298, P_{1V} = -11.460 \quad (3.7a)$$

$P_{2H} = 20.048, P_{2V} = 17.514$ (3.7b)

$P_{3H} = 10.000, P_{3V} = 10.000$ (3.7c)

$P_{4H} = 4.529, P_{4V} = 4.891$ (3.7d)

$P_{5H} = 2.927, P_{5V} = 3.135$ (3.7e)

$P_{6H} = -1.173, P_{6V} = -0.888$ (3.7f)

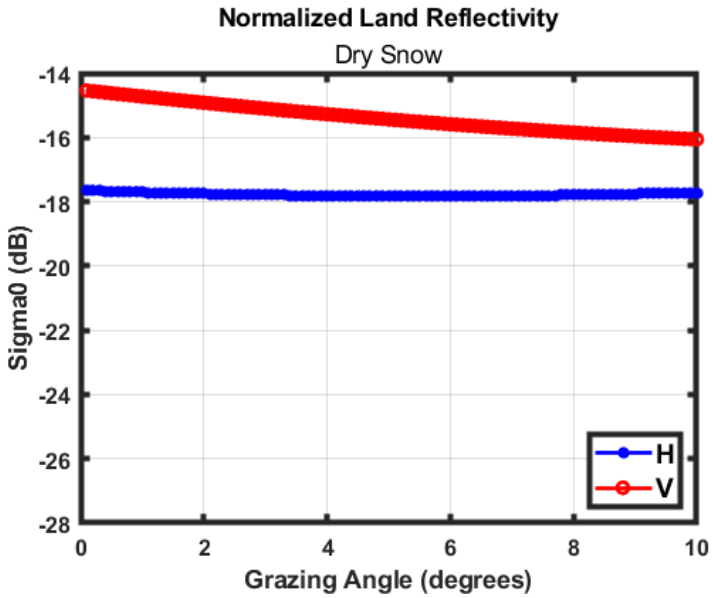

Figure 3.6. Land clutter normalized RCS at 10 GHz as a function of grazing angle from the Ulaby and Dobson model for dry snow.

Figure 3.6 shows that vertically polarized waves have more reflectivity than horizontally polarized waves for $0.1^{\circ} - 10^{\circ}$ grazing angles.

3.1.7. Wet snow

Wet snow has a LWC larger than 1 percent of its volume.

Parameters of the model for X-band:

$P_{1H} = 10.020, P_{1V} = 10.952$ (3.8a)

$$P_{2H} = 7.909, P_{2V} = 6.473 \quad (3.8b)$$

$$P_{3H} = 15.000, P_{3V} = 15.000 \quad (3.8c)$$

$$P_{4H} = 30.000, P_{4V} = 30.000 \quad (3.8d)$$

$$P_{5H} = 0.828, P_{5V} = 0.777 \quad (3.8e)$$

$$P_{6H} = 2.073, P_{6V} = 2.081 \quad (3.8f)$$

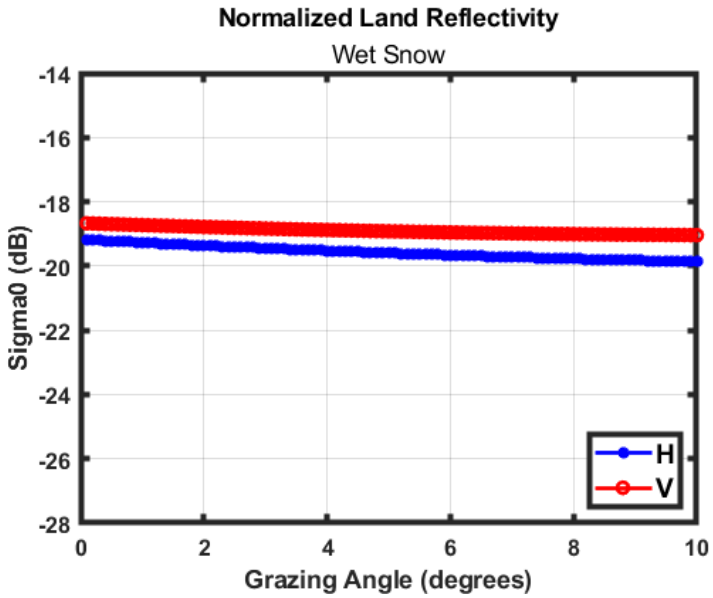

Figure 3.7. Land clutter normalized RCS at 10 GHz as a function of grazing angle from the Ulaby and Dobson model for wet snow.

Figure 3.7 shows that vertically polarized waves have more reflectivity than horizontally polarized waves for $0.1^{\circ} - 10^{\circ}$ grazing angles.

Land clutter σ^0 values are given in Table 3.1. The average clutter of the horizontal polarization wave of seven land types is $-19.74\ dB$ at the 10° grazing angle. Moreover, the average vertical polarization is $-18.95\ dB$ at the 10° grazing angle.

The average clutter of the horizontal polarization is $-21.46\ dB$, and the average clutter of the vertical one is $-20.79\ dB$ at the 1° grazing angle.

The average clutter of the horizontal polarization is $-21.63\ dB$, and the average clutter of the vertical one is $-20.97\ dB$ at the 0.1° grazing angle.

Horizontal polarization leads to less clutter than the vertical one for all grazing angles on average as shown in Figure 3.8. It is an expected result that the average clutter of vertical polarization is stronger than horizontal polarization [30].

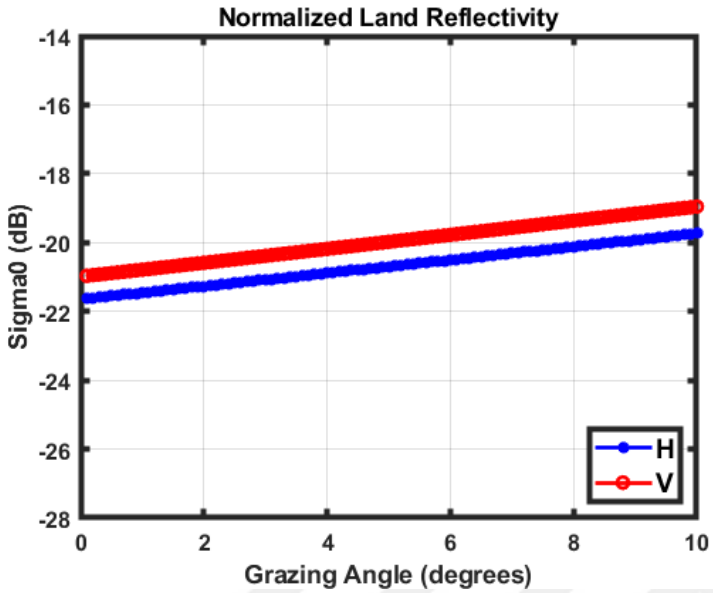

Figure 3.8. Average land clutter normalized RCS at 10 GHz vs grazing angle

Table 3.1. Land clutter for seven land types and $0.1^{\circ} - 10^{\circ}$ grazing angles (in dB)

Land Type	Soil and Rock	
Polarization	H	V
Grazing angle		
0.1°	-17.49	-26.79
1°	-17.49	-26.34
10°	-17.25	-21.83
	Grass	
0.1°	-18.20	-17.19
1°	-17.98	-17.00
10°	-15.94	-15.35
	Shrub	
0.1°	-16.99	-17.87
1°	-16.81	-17.69
10°	-15.00	-15.73
	Short Vegetation	
0.1°	-17.66	-18.68
1°	-17.45	-18.44
10°	-15.37	-16.00
	Road Surface	
0.1°	-44.21	-33.03
1°	-43.50	-32.60
10°	-37.01	-28.66
	Dry Snow	
0.1°	-17.65	-14.54
1°	-17.71	-14.72
10°	-17.71	-16.06
	Wet Snow	
0.1°	-19.19	-18.67
1°	-19.27	-18.73
10°	-19.87	-19.04

4. COMPARISON OF SEA AND LAND CLUTTER

In this part of the thesis, sea and land clutter results are compared for $0.1^{\circ} - 10^{\circ}$ grazing angle. While comparing, mean sea clutter value is used, and it is compared with seven land clutter results that are calculated in third chapter. Comparisons in terms of horizontal polarization are given in given in Figure 4.1 – Figure 4.7. In addition, comparisons in terms of vertical poarization are given in Figure 4.7 – Figure 4.14. Finally, results are given numerically in Table 4.1.

4.1. Comparison According to Horizontal Polarization

In Figure 4.1, the road surface has more clutter between $0.1^{\circ} - 0.6^{\circ}$ grazing angle. However, the mean sea clutter is more than the clutter of the road surface for the grazing angle range of $0.6^{\circ} - 10^{\circ}$. For the comparisons of wet snow, grass, short vegetation, dry snow, soil and rock, and shrub, land clutter is more than the mean sea clutter for the whole grazing range of calculation, i.e., $0.1^{\circ} - 10^{\circ}$. They are shown in Figure 4.2 – Figure 4.7, respectively.

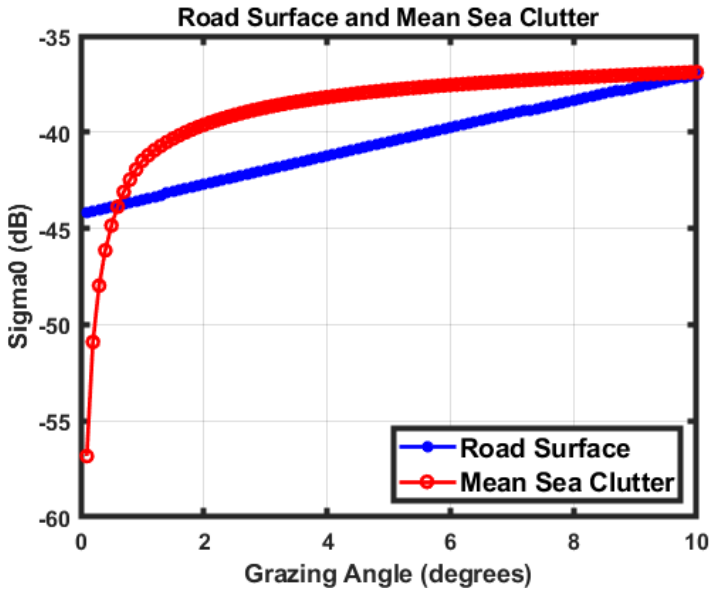

Figure 4.1. Comparison of road surface and mean sea clutters at 10 GHz as a function of grazing angle for horizontal polarization.

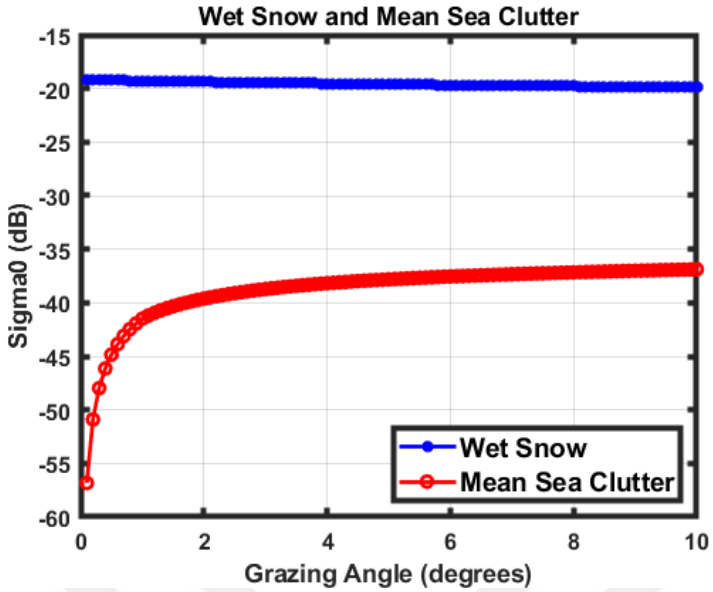

Figure 4.2. Comparison of wet snow and mean sea clutters at 10 GHz as a function of grazing angle for horizontal polarization.

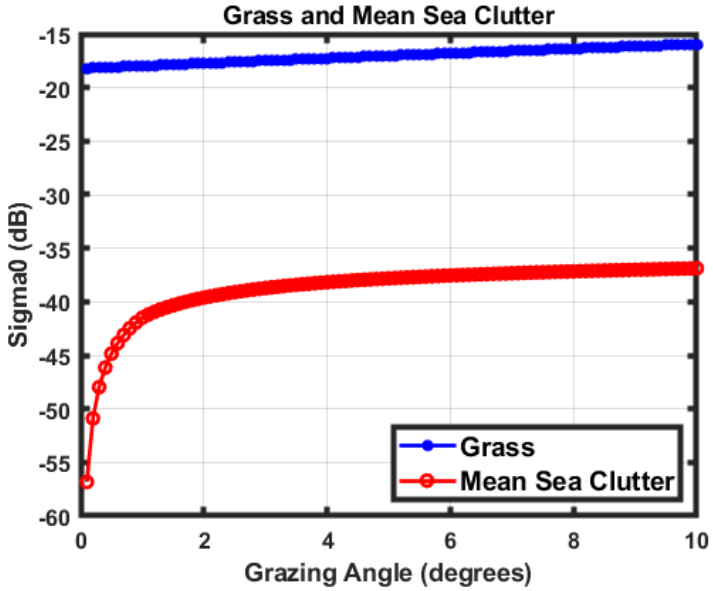

Figure 4.3. Comparison of grass and mean sea clutters at 10 GHz as a function of grazing angle for horizontal polarization.

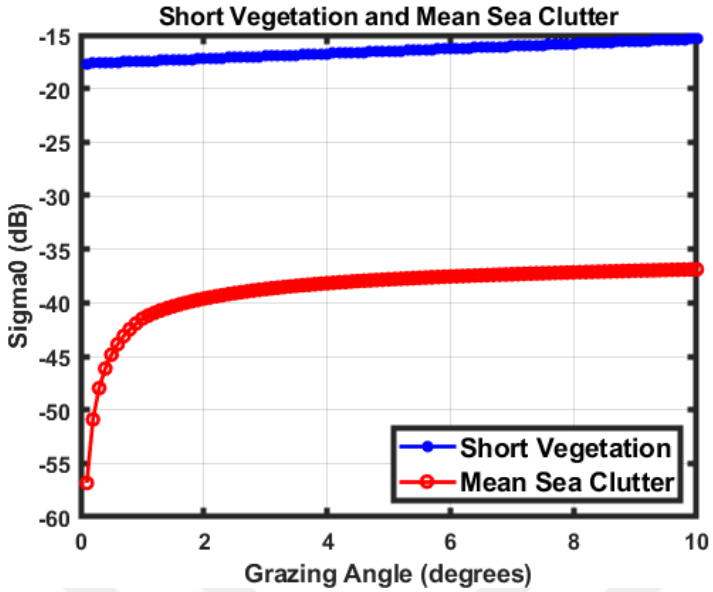

Figure 4.4. Comparison of short vegetation and mean sea clutters at 10 GHz as a function of grazing angle for horizontal polarization.

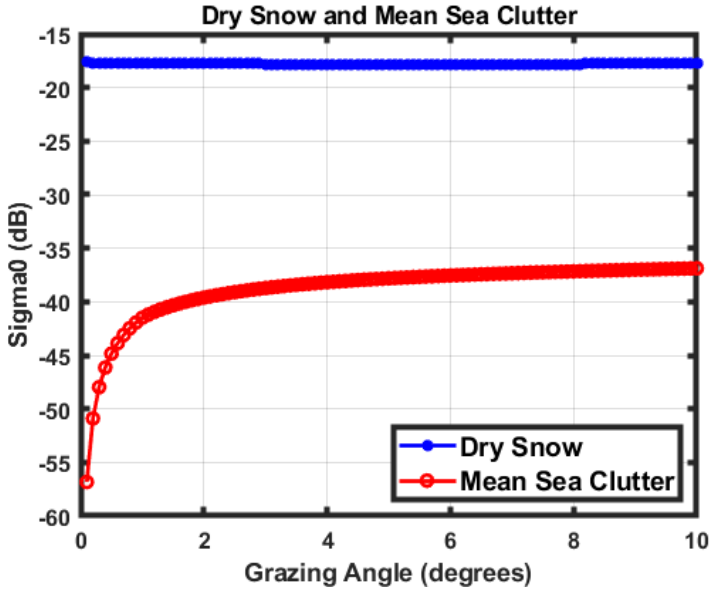

Figure 4.5. Comparison of dry snow and mean sea clutters at 10 GHz as a function of grazing angle for horizontal polarization.

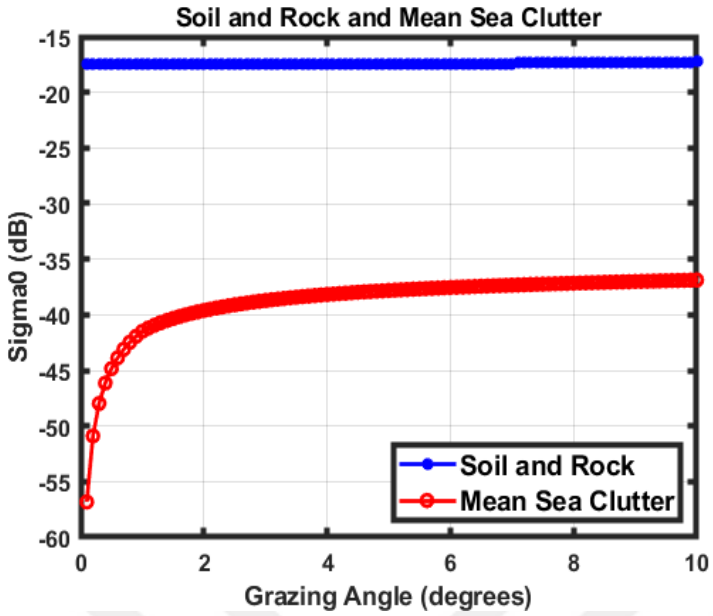

Figure 4.6. Comparison of soil and rock and mean sea clutters at 10 GHz as a function of grazing angle for horizontal polarization.

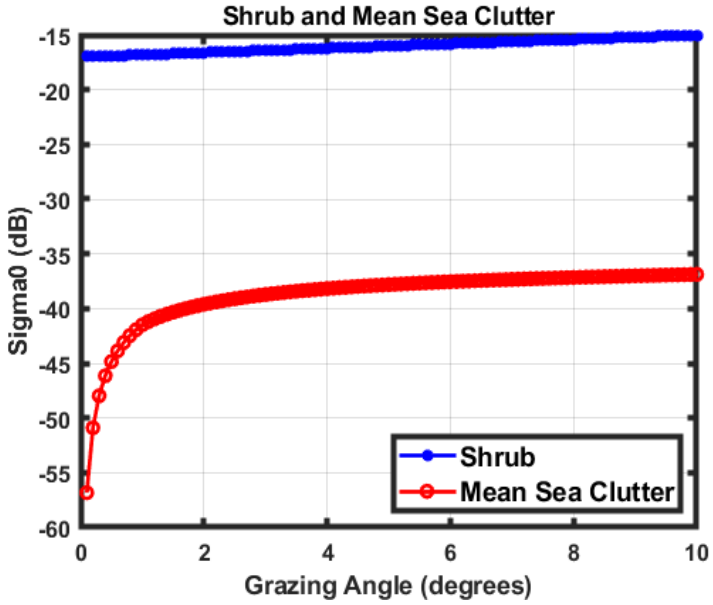

Figure 4.7. Comparison of shrub and mean sea clutters at 10 GHz as a function of grazing angle for horizontal polarization.

4.2. Comparison According to Vertical Polarization

In Figure 4.8 – Figure 4.14, the mean sea clutter is less than land clutter for all types of road surface, wet snow, grass, short vegetation, dry snow, soil and rock, and shrubs. This result is valid for all of the calculation ranges, i.e. $0.1^{\circ} - 10^{\circ}$ grazing angle.

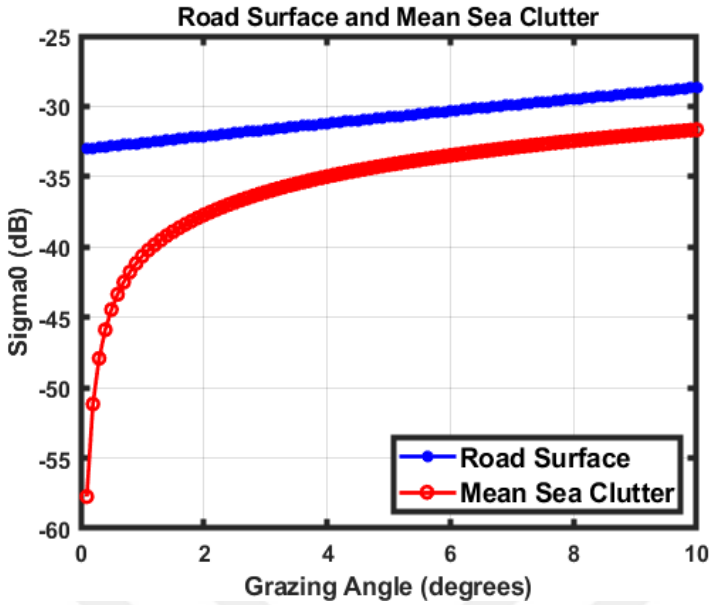

Figure 4.8. Comparison of road surface and mean sea clutters at 10 GHz as a function of grazing angle for vertical polarization.

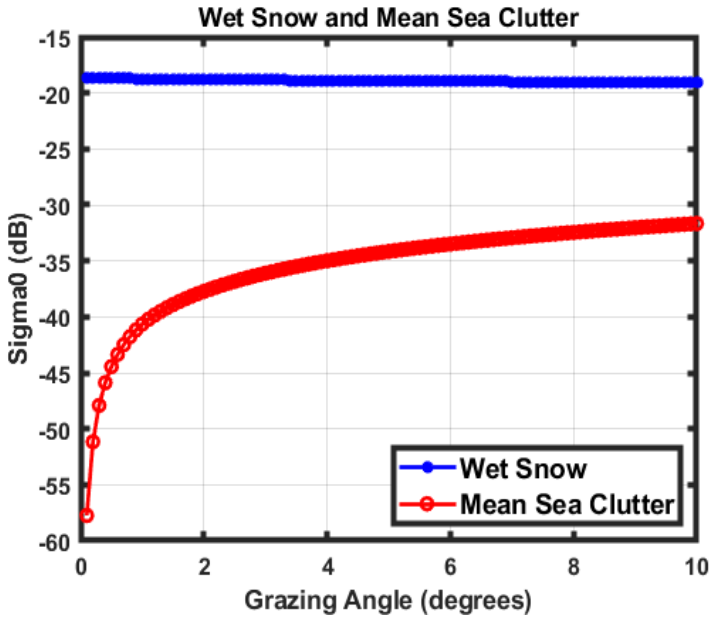

Figure 4.9. Comparison of wet snow and mean sea clutters at 10 GHz as a function of grazing angle for vertical polarization.

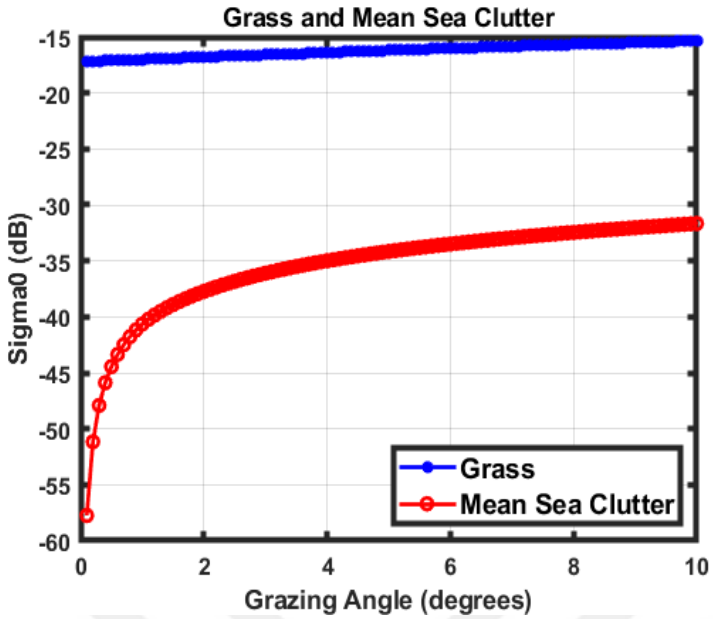

Figure 4.10. Comparison of grass and mean sea clutters at 10 GHz as a function of grazing angle for vertical polarization.

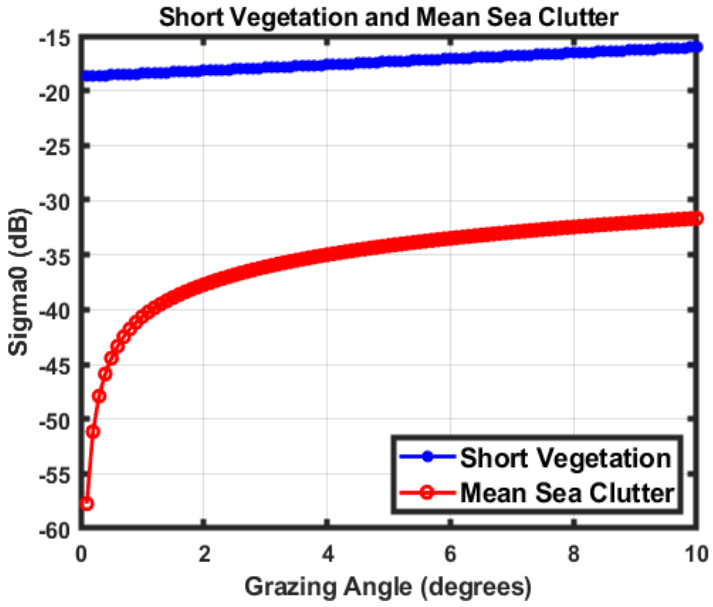

Figure 4.11. Comparison of short vegetation and mean sea clutters at 10 GHz as a function of grazing angle for vertical polarization.

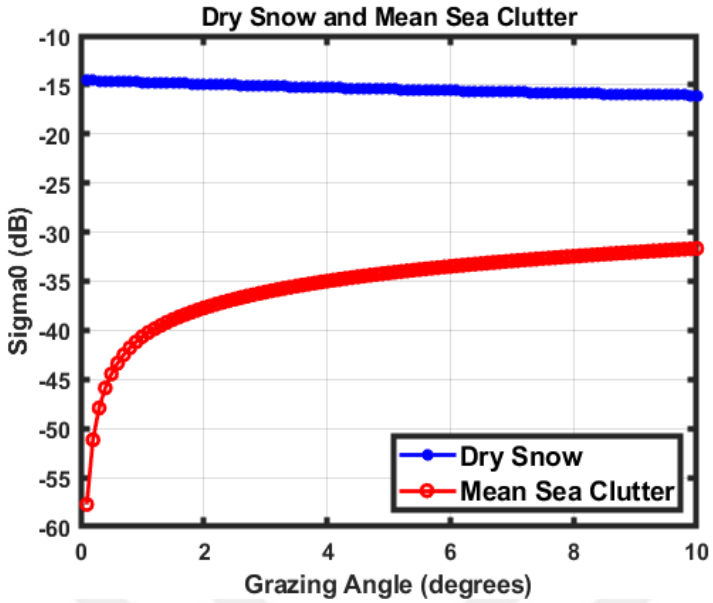

Figure 4.12. Comparison of dry snow and mean sea clutters at 10 GHz as a function of grazing angle for vertical polarization.

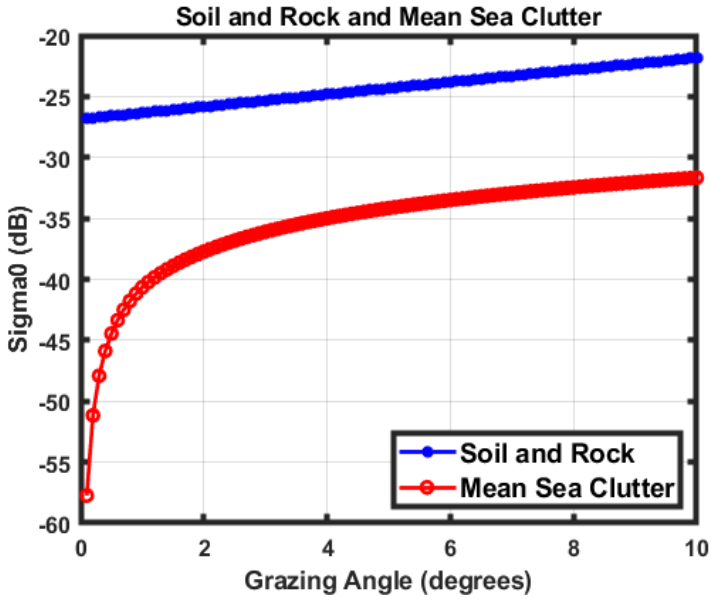

Figure 4.13. Comparison of soil and rock and mean sea clutters at 10 GHz as a function of grazing angle for vertical polarization.

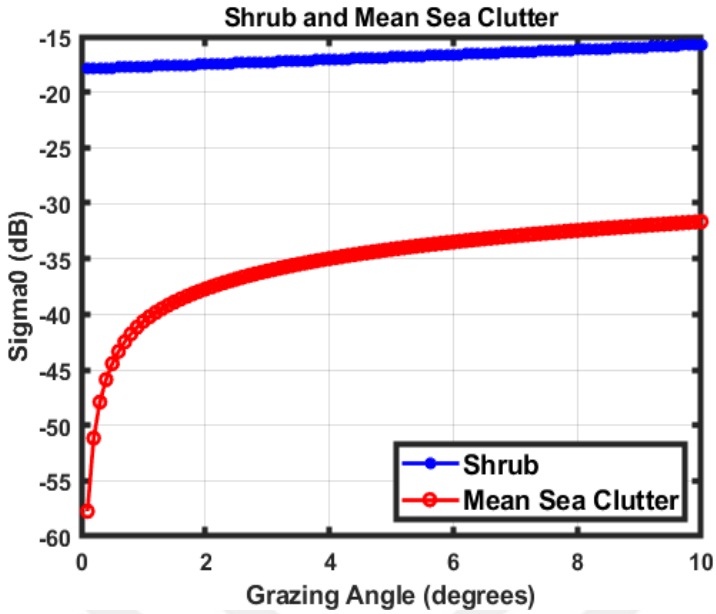

Figure 4.14. Comparison of shrub and mean sea clutters at 10 GHz as a function of grazing angle for vertical polarization.

When land and average sea clutters are compared using Table 4.1, it can be understood that land clutter is more than sea clutter. It is an expected result as indicated in the Massachusetts Institute of Technology (MIT) lecture [31]. The indication is that mean sea clutter is about a hundred times in linear scale, i.e., 20 dB in dB scale, less than the land clutter. Average sea clutters are calculated using four models, and mean sea clutter is calculated using six sea states.

Table 4.1. Comparison of land and average sea clutters for horizontal and vertical polarizations and $0.1^{\circ} - 10^{\circ}$ grazing angles (in dB).

Grazing angle	0.1°		1°		10°	
Polarization	H	V	H	V	H	V
Sea State 1	-81.215	-78.123	-51.358	-48.883	-46.793	-40.053
Sea State 2	-67.103	-65.525	-53.050	-50.985	-40.460	-34.725
Sea State 3	-57.410	-57.710	-40.910	-39.863	-37.075	-31.700
Sea State 4	-50.733	-52.088	-37.215	-36.950	-34.458	-29.503
Sea State 5	-44.715	-47.900	-34.355	-34.525	-32.168	-27.663
Sea State 6	-40.238	-44.680	-32.025	-32.685	-30.383	-26.318
Mean Sea Clutter	-56.902	-57.671	-46.319	-40.649	-36.890	-31.660
Road Surface	-44.21	-33.03	-43.50	-32.60	-37.01	-28.66
Wet Snow	-19.19	-18.67	-19.27	-18.73	-19.87	-19.04
Grass	-18.20	-17.19	-17.98	-17.00	-15.94	-15.35
Short Vegetation	-17.66	-18.68	-17.45	-18.44	-15.37	-16.00
Dry Snow	-17.65	-14.54	-17.71	-14.72	-17.71	-16.06
Soil and Rock	-17.49	-26.79	-17.49	-26.34	-17.25	-21.83
Shrub	-16.99	-17.87	-16.81	-17.69	-15.00	-15.73

5. CONCLUSION

In this thesis sea and land clutter are calculated for two polarizations which are vertical and horizontal. To calculate sea clutter four models are used which are RRE, GIT, Proposed, and NRL models. In addition, to calculate land clutter the Ulaby and Dobson model is used, and clutter is calculated for different land types which are soil and rock, grass, shrub, short vegetation, road surfaces, dry snow, and wet snow. Clutter is symbolized with σ^0, and shown in dB on result graphs. Calculations are made for the $0.1^\circ - 10^\circ$ grazing angle range, and 10 GHz frequency. Also, MATLAB is used to calculate and visualize the results.

In the second chapter, sea clutter is calculated for six sea states by using four different models. Then models and sea states are compared. The main finding is horizontal polarization has less clutter than vertical polarization. This result is an expected result as indicated in [16]. Also, the effect on the range increase of clutter difference is calculated. The second finding is that sea clutter is increasing as sea state increases. The third finding is as the grazing angle increases sea clutter is also increasing.

In the third chapter, land clutter is calculated for seven land types. Then, numerical values are compared in terms of polarization. The main result is horizontal polarization has less clutter than vertical one. It is an expected result from [30].

In the fourth chapter, land and mean sea clutter are compared. Mean sea clutter is calculated by averaging all calculated values for sea states and models in the second chapter. The result of the comparison is that land clutter is more than the mean of sea clutter. It is also an expected result from [31].

In conclusion, a dual-polarized antenna allows to get different clutter by using vertical and horizontal polarizations. Since radar systems can increase target detection range by using polarization that has smaller clutter, it can be used in radar systems. Several examples that used dual-polarized antenna are given in practical applications such as CAMRa and WR120. Also, some examples that used horizontal-polarized antenna are given in practical applications such as RADARSAT-1, RM-1290, and FINO-I.

This thesis is different from the other studies in that it uses four different models to calculate sea clutter in terms of sea state, grazing angle, and polarization. The second difference is that it compares land and average sea clutter.

For future work, a researcher could measure sea and land clutter, and compare the measurements with calculations. Then, one model could be chosen or developed that is compatible with measurements.

REFERENCES

1. Internet: Schweber, B. (July, 2022). Antenna polarization: What It Is and Why It Matters. *DigiKey*. Web: https://www.digikey.com/en/blog/antenna-polarization-what-it-is-and-why-it-matters Date of access: 21.01.2024.

2. Balanis, C. A. (2005). *Antenna Theory Analysis and Design.* (3^{rd} Edition). New Jersey: John Wiley & Sons Inc., 70-80.

3. Internet: Dong, Y. (September, 2004). Models of Land Clutter vs Grazing Angle, Spatial Distribution and Temporal Distribution - L-Band VV Polarisation Perspective. *Defense Technical Information Center*. Web: https://apps.dtic.mil/sti/pdfs/ADA426119.pdf/ Date of access: 27.01.2024.

4. Internet: Sjöberg, D. (October, 2020). EITN90 Radar and Remote Sensing Lecture 4: Characteristics of Clutter. *Department of Electrical and Information Technology*. Web: https://www.eit.lth.se/fileadmin/eit/courses/eitn90/2020/lectures/lecture4.pdf Date of access: 09.02.2024.

5. Internet: Tomlinson, P. G. (August, 2011). A model for space radar clutter. *Defense Technical Information Center*. Web: https://apps.dtic.mil/sti/tr/pdf/ADA072990.pdf Date of access: 20.01.2024.

6. Internet: Maritime Surveillance Radar. I. Radar scattering from the ocean surface. (1990). IEEE Proceedings Radar and Signal Processing, 137 (2). Web: https://ieeexplore.ieee.org/document/216955/ Date of access: 05.03.2024.

7. Özbaş, E. (2021). *Modeling Monostatic Sea Clutter at Low Grazing Angles by Using Method of Moments.* Masters's Thesis, The Graduate School of Natural and Applied Sciences of Middle East Technical University, Ankara, 13-15.

8. Internet: Greco, M. S. (n.d.). Radar Clutter Modeling. *uniPi*. Web: http://docenti.ing.unipi.it/m.greco/esami_lab/Radar/Clutter_modeling.pdf Date of access: 10.03.2024.

9. Watts, S. (2013). *The Modelling of Radar Sea Clutter*. Doctor of Science. The School of Electronic, Electrical and Computer Engineering University of Birmingham, Birmingham, 6-8.

10. Greco, M. S. and Watts, S. (2014). *Radar Clutter Modeling and Analysis.* (2^{nd} Edition). Pisa: Academic Press, 513–594.

11. Thottempudi, P. (2013). *Generation and Simulation of Clutter for Radar Testing Using FPGA*. Master of Technology, Science, Technology and Research Deemed University, Guntur, 20.

12. Skolnik, M. I. (2001). *Introduction to Radar Systems* (3^{rd} Edition). Singapore: McGraw-Hill, 403–481.

13. Internet: Eastment, J. D. (April, 1994). CAMRA radar. *Science & Technology Facilities Council.* Web: https://www.chilbolton.stfc.ac.uk/Pages/CAMRa.pdf Date of access: 17.11.2023.

14. Internet: (2020). Compact X-band Dual Polarimetric Doppler Weather Radar. *Furuno.* Web: https://www.furuno.com/en/systems/meteorological-monitoring/WR2120 Date of access: 18.11.2023.

15. Internet: Skålvik, T. (December, 2022). Benefits of a dual-polarization weather radar. *Furuno.* Web: https://www.furuno.no/en/weather-radar-knownledge/benefits-of-dual-polarization-radar/ Date of access: 19.11.2023.

16. Internet: (November, 2014). Ship Detection. Web: https://natural-resources.canada.ca/maps-tools-and-publications/21448 Date of access: 24.11.2023.

17. Wang, H., Qiu, H., Zhi, P., Wang, L., Chen, W., Akhtar, R., and Zahoor Raja, M. A. (2019). Study of algorithms for Wind Direction Retrieval from X-band Marine Radar Images. *Advanced Technology Related to Radar Signal, Imaging, and Radar Cross-Section Measurement*, 8(7), 764–785.

18. Dankert, H. and Horstmann, J. (2005). Wind measurements at FINO-I using marine radar-image sequences. *2005 IEEE International Geoscience and Remote Sensing*, 4777-4780.

19. Dankert, H., and Horstmann, J. (2007). A Marine Radar Wind Sensor. *Journal of Atmospheric and Oceanic Technology*, *24*(9), 1629–1642.

20. Nathanson, F.E. (1969). *Radar design principles.* (2^{nd} Edition). New York: McGraw-Hill, 274-280.

21. Daley, J. C., Ransone, J. T., Burkett, J. A., and Duncan, J. R. (Naval Research Laboratory). (1968). *Sea clutter measurements on four frequencies. NRL.* Washington, 6-44.

22. Ward, K. D., Tough, R. J. A., and Watts, S. (2006). *Sea Clutter: Scattering, the K Distribution and Radar Performance.* (1^{th} Edition). United Kingdom: The Institution of Engineering and Technology, 233–236.

23. Watts, S., Ward, K., and Greco, M. (2016, 13 July). *Radar Performance in Clutter - Modelling, Simulation and Target Detection Methods.* The 13^{th} European Radar Conference, London.

24. Chen, Z., Liu, X., and Wang, X. (2013). *The analysis of sea clutter statistics characteristics based on the observed sea clutter of Ku-band Radar.* 2013 Proceedings of the International Symposium on Antennas & Propagation, China, 1183-1186.

25. Gregers-Hansen, V., and Mital, R. (2012). An improved empirical model for radar sea clutter reflectivity. *IEEE Transactions on Aerospace and Electronic Systems*, *48*(4), 3512–3524.

26. Gregers-Hansen, V. and Mital, R. (Naval Research Laboratory.). (2012). An Improved Empirical Model for Radar Sea Clutter Reflectivity. *NRL*. Washington, 1-12.

27. Gregers-Hansen, V. and Mital, R. (2009). *An Empirical Sea Clutter Model for Low Grazing Angles.* 2009 IEEE Radar Conference, California, 1-5.

28. Richards, M. A. (2014). *Fundamentals of Radar Signal* Processing (2^{nd} Edition). New York: Mc Graw Hill Education, 89-180.

29. Ulaby, F. and Dobson, M. C. (2019). *Handbook of Radar Scattering Statistics for Terrain.* (1^{th} Edition). Massachusetts, 119-357.

30. Billingsley, J. B. (2002). *Low-Angle Radar Land Clutter: Measurements and Empirical Models.* (1^{th} Edition). New York: SciTech Publishing Inc., 143–284.

31. Internet: O'Donnell, R. M. (February, 2024). Radar Clutter and Chaff. Massachusetts Institute of Technology Lincoln Laboratory. Web: https://www.ll.mit.edu/outreach/radar-introduction-radar-systems-online-course. Date of access: 05.02.2024.

Gazili olmak ayrıcalıktır